NASA Contractor Report 174639

Literature Survey on Oxidations and Fatigue Lives at Elevated Temperatures

H. W. Liu and Y. Oshida

Syracuse University
Syracuse, New York

March 1984

Prepared for

NATIONAL AERONAUTICS AND SPACE ADMINISTRATION
Lewis Research Center
Under Grant NAG 3-348

CONTENTS

I. INTRODUCTION

Fatigue lives at elevated temperatures are often shortened by creep and/or oxidation. Creep deformation creats voids and weakens the material. In conjunction with cyclic load, creep damage may accelerate the initiation and growth of fatigue cracks. Oxides are brittle solids that have very low fracture strength and fracture toughness. Therefore, oxidation also accelerates fatigue damage both in terms of fatigue crack initiation and fatigue crack propagation. There is a considerable amount of information on creep and fatigue interaction and their acceleration of fatigue damage.[1] This review, however, concentrates on oxidation effects on fatigue damage.

It is well known that the data scatter band of stage II fatigue crack growth is very narrow. Therefore, the wide scatter of fatigue lives might be due to the large scatter in fatigue crack initiation and possibly due to the scatter in stage I crack growth.[2] The crack initiation period could be shortened considerably by the fractures of carbides and intermetallic compounds or by grain boundary oxidation. The oxidation accelerated fatigue crack initiation may contribute to the scatter of fatigue lives.

Bricknell and Woodford[3] observed embrittlement as a reduction of the tensile elongation of nickel and nickel alloys due to high-temperature oxidation. They tested three grades of nickel (Ni200, Ni270, and Spec-pure Ni) following air exposure at 1000°C. Tests in a variety of gaseous conditions have revealed oxygen as the damaging species and have shown that even low partial pressures of oxygen can result in considerable decrease in tensile elongation.

Cyclic deformation significantly increases the oxidation rate.[4] Coffin[5] also observed the inability of a film to provide protection against oxidation wherever a highly localized deformation occurs. The repeated rupture of the oxide film during a fatigue test results in the extremely high oxidation rate in these localized regions. Cyclic stress or strain comes from either mechanical or thermal effects. Thermal stresses arise from temperature gradient due to transient temperature fluctuation and the mismatch of the thermal coefficients of the surface oxide and the substrate.

Coffin et al.[6] have studied cast Udimet 500 subjected to low-cycle fatigue at 1500°F (815°C) and showed the fatigue crack initiation to be the result of a localized ridging. Crack propagation occurs along grain boundaries accompanied

by substantial amounts of oxidation. Coffin et al. proposed a "stress oxidation" mechansim for crack initiation and propagation, especially along grain boundaries. The presence of oxide-filled intergranular cracks is a common observation at high temperatures. It is clear that oxidation may shorten the fatigue life considerably. However, a detailed quantitative relation between oxidation and fatigue life is still lacking.

This literature survey relevant to high-temperature low-cycle fatigue in nickel-base superalloys reviews general oxidation, selective oxidation, internal oxidation, grain boundary oxidation, multi-layer oxide structure, accelerated oxidation under stress, stress-generation during oxidation, composition and substrate microstructural changes due to prolonged oxidation, fatigue crack initiation at oxidized grain boundaries and the oxidation accelerated fatigue crack propagation along grain boundaries.

II. OXIDATION OF Ni AND Ni-BASE SUPERALLOYS

Nickel-base superalloys are the most complex and the most widely used for high-temperature applications. The required properties of nickel-base superalloys for applications such as aircraft engine components are high-temperature tensile strength, thermomechanical fatigue resistance, low thermal expansion, as well as oxidation resistance. Oxidation behavior of the nickel-base superalloys is extremely complex for the following reasons.

1). Each alloying element has different affinity for oxygen. Since the affinity in metal/oxide reactions is nearly proportional to the heats of decomposition of oxides per mole of oxygen,[7] one may estimate the ease of oxide formation of each alloying element by comparing the ΔH_{dec} (heats of decomposition) data listed in Table 1,[8] because the higher the ΔH_{dec}, the more stable the oxide. Table 1 shows that oxides of chromium and aluminum form more readily than oxides of other major alloying elements. NiO is also formed because Ni is the major constituent of the alloy. The oxides of tantalum, silicon, and zirconium are seldom formed, even though they are stable oxides, because Ta, Si, and Zr are minor constituents.

Depending on the affinity of an element for oxygen and the stability of its oxide, one or two of the alloying constituents are selectively oxidized. Generally any alloy containing a small quantity of a metal (which has a high affinity for oxygen, forms an oxide showing resistance to diffusion of oxygen and the solute atoms, and has little solubility in the oxide of the solvent metal) should have a strong oxidation resistance if the oxide film has a strong adherence to the substrate.[9]

At a reduced partial pressure of oxygen, that is, under conditions of limited availability of oxygen at the surface, oxidation is selective.[10] A lower partial pressure of oxygen will also develop at the protective external scale/metal interface. Therefore, if a metal is covered with a dense, protective oxide film (or scale) adhering tightly to metal substrates, then selective oxidtaion will occur at the oxide/metal interface.

2). Since the oxides formed on nickel-base superalloys are not single phase, there might exist a solid-state reaction among these oxides. If they are mutually insoluble, a complex structure of oxides might result (such as double layers or multi-layers of external oxides). The formation of complex oxides will be a function of alloy composition, temperature, oxygen pressure, and oxidation time.[11]

Figure 1 shows an example of the complex oxides formed on (a) René 41 (19% Cr, 11%Co, 10%Mo, 3.1%Ti, 1.5%Al, and 0.7%Fe) and (b) Udimet 700 (15%Cr, 19%Co, 5%Mo, 3.5%Ti and 4.5%Al).[10] The kinetics of the reaction and the main reaction products change with temperature and oxidation time. Hence, at the early stage of oxidation, the growth rate of oxide is predominantly linear. The rate determining process involves the transport of the reactants of the oxidation process.[12] By continuing the oxidation or by increasing the thickness of the oxide film (or scale), diffusion becomes the rate controlling process and the growth rate becomes parabolic, as discussed below.

Let us consider the complex oxide structure and composition, which is more common in Ni-Cr-Co-Mo-Ti-Al alloys. Suppose the external oxide scale consists of NiO, Cr_2O_3, Al_2O_3, $(Cr,Al)_2O_3$, $NiCr_2O_4$, $NiAl_2O_4$, $Ni(Cr,Al)_2O_4$ and TiO_2 and the internal oxide subscale includes Al_2O_3. Then, as shown in Figure 2, the following steps occur. (a) At an early stage of oxidation, a compact NiO layer is formed because Ni is the major constituent.

(b) As the oxidation proceeds, a porous NiO layer forms beneath the compact NiO layer. However, the total NiO layer thickness is increasing because the diffusion rate of Ni in NiO is higher than that of Cr in Cr_2O_3, as will be discussed later. At the same time, Cr_2O_3 and Al_2O_3 oxides form at the interface of the inner porous NiO layer and the substrate. The rapid diffusion of the nickel atoms toward the outer surface causes the porous structure. The inward diffusion of oxygen toward the substrate and the reaction of the oxygen with chromium result to form Cr_2O_3. Some of these oxides may be formed inside the porous NiO layer, resulting in a solid-state reaction to form a spinel-type oxide such as $NiCr_2O_4$, $NiAl_2O_4$, or a mixture of the two as $Ni(Cr,Al)_2O_4$.

(c) As the oxidation proceeds further, more spinel-type oxides may be formed and small particles of Al_2O_3 will be formed as a subscale beneath the metal surface.

(d) By increasing the thickness of both external and internal scales, TiO_2 will be formed at the scale/substrate interface because Ti is enriched relatively to the other elements, which are already depleted through oxidation.

3). When oxygen dissloves in the alloy phase during oxidation, the less noble alloy component may form small oxide particles within the alloy, as shown in Figure 2 (c), and bands of oxide may form beneath the external scale/alloy interface. This type of scale is known as subscale and the process is called internal oxidation.

4). In some cases, liquid oxide phases may also formed on a surface. This may occur (i) if materials are exposed to the vapor of a low-melting oxide during oxidation or (ii) in oxidation of alloys with an alloying component that forms a low-melting oxide. The typical low-melting oxides are MoO_3(m.p.: 795°C) and V_2O_5 (m.p.: 674°C).[13] The presence of liquid oxide phases may lead to excessively fast oxidation and disintegration of the alloy. This phenomenon is commonly termed catastrophic oxidation, often occurs in boiler or superheater tubes where the combustion gas contains V_2O_5, which condenses and reacts with fly ash and oxide scales on the heat exchanger tubes. This process is also known as V-attack (i.e. the vanadium-attack). An analogous phenomenon may exist in the case of the volatile oxide CrO_3. The CrO_3 oxide forms in the temperature range 950°C - 1020°C.[14,15,16] Although the vapor pressure of CrO_3 is usually low in this temperature region, it is volatile at such high temperatures.

Selective oxidation, growth of oxides, reaction between different oxides, and internal oxidation are always observed in nickel-base superalloys to a certain extent depending on chemical compositions, temperature, oxygen pressure, and time of oxidation.

Before discussing the kinetics of oxidation, let us summarize the alloying effects of individual constituents in nickel-base superalloys.

Chromium: 1) Chromium appears to be an obvious choice for high-temperature alloying constituent by virtue of a natural protective layer of chromic oxide (Cr_2O_3) which adheres to a surface.[17]

2) The "critical" minimum content of chromium to ensure the formation of a protective Cr_2O_3 scale is approximately 15%[18] or 20 - 25%.[19,20,21]

3) For these alloys, a thin external NiO layer is formed by rapid overgrowth during the early stage. Under this layer is the protective Cr_2O_3 layer, which controls the oxide growth, as an intermediate spinel-type oxide layer (such as nickel chromite: $NiCr_2O_4$) often does.[22,23]

Cobalt: 1) Cobalt (as well as Ni, Fe, Cr, Mo, W, and V) is an austenitic former element and it enhances the γ-phase formation. Cobalt is a weak solid solution strengthener.[24]

2) improves the creep strength.[17,25]

3) raises the solvus temperature of γ'-phase, $Ni_3(Al,Ti)$.[26]

Molybdenum:

1) improves the creep strength.[17]

2) Molybdenum (as well as Cr and W) is one of the best substitutional solid solution strengtheners.[19]

Tantalum:

1) improves the creep resistance.[27]

Niobium:

1) Niobium (as well as Ti and Ta) substitutes for Ni in Ni_3Al type γ' precipitate.[24]

2) Niobium (as well as Cr, Mo, W, V, Ta, and Ti) is an effective carbide former ($M_{23}C_6$, M_6C, MC).[19]

Zirconium:

1) Zirconium (as well as Th, Ce, and Ca) is effective to produce the protective oxide film (or scale) due to the "keying" effect for anti-spalling.[28,29]

2) promotes ductility.[26]

Manganese:

1) improves the strength as a solid solution metal in Ni without appreciable reduction of ductility.[25]

Boron: 1) segregates to grain boundaries and improves creep properties (by decreasing elongation and increasing rupture stress).[24]

Aluminum:

1) increases the oxidation resistance by formation of continuous Al_2O_3 layer.[20]

2) Aluminum (as well as Cr) is one of the best substitutional solid solution strengtheners.[19]

Chromium and Alminum:

1) Simultaneous additions of Cr and Al to Ni produce a protective complex oxide structure of NiO, Cr_2O_3, and Al_2O_3 and their spinel type mixed oxides such as $NiCr_2O_4$, $NiAl_2O_4$, and $Ni(Cr,Al)_2O_4$.[30, 31,32,33,34] This oxide gives rise to high oxidation resistance.[20]

2) The Cr/Al ratio plays an important role in the types of oxide formed.[30,31]

(i) For both low Cr and Al contents, an external NiO scale forms over internal scales of Cr_2O_3 and Al_2O_3,

(ii) For high Cr (>15%) but low Al (<3%) contents, both Cr_2O_3 and Al_2O_2 have been observed as external oxides, and

(iii) For relatively high Cr (>15%) and high Al (>3%) contents, an exclusive Al_2O_3 scale is formed.

When nickel is heated in oxygen, it forms an adherent film scale of nickel oxide, NiO, which controls the rate of further oxidation by acting as a diffusion barrier between the metal and the atmosphere. The mechanism and the rate-controlling process for the initial formation of the film and its growth at relatively low temperatures (i.e., below $400^{\circ}C$), are not at all clearly understood, but at higher temperature the growth follows a parabolic law.

Wagner's mechanism[35] for the parabolic relationship is that of film thickening controlled by diffusion due to a concentration gradient. Since the oxide film is composed of cations (metal ions) and anions (oxygen ions), this diffusion across the film must be accompanied by a simultaneous diffusion of electrons in the same direction as the cations, or in the opposite direction to the anions. Hence the oxidation of nickel is governed by the diffusion (as a rate-determining factor) of charged vacancies in the oxides or of only one type of ion (either cation or anion) or of electron through the lattice defects of oxides.

Methods of investigating the growth of oxide layers include determination of changes in thickness of the scale, in weight of the metal sample, or in volume of the surrounding gas.[36] Most quantitative data have been obtained as changes in weight (ΔW) per unit surface area. Kinetic theory is concerned primarily with the progress of a reaction with time. Thus, the first task is to find relationship between oxidation and time t. The parabolic relationship of the oxidation process $(\Delta W)^2 = a \times t$ represents a straight line when $(\Delta W)^2$ is plotted against time t. If this line does not intersect the origin of the coordinate axes, the more general form of the parabolic equation, $(\Delta W)^2 = a \times t + C$, is applicable. The constant a in the above equations is the parabolic rate constant.

Figure 3 shows the self-diffusion coefficients of a metal ion (cation) in its single or complex oxides. Figure 4 shows the parabolic rate constant of

several nickel-base superalloys.

It is well known that the temperature dependence of reaction rates is governed by an exponential relation known as the Arrhenius equation. According to this equation, the temperature dependence of diffusion rates is generally written in the form $D = D_o e^{-Q/RT}$, where D_o and Q are constants. On the other hand, according to Kubaschewski and Hopkins;[37] the temperature-dependent parabolic rate constant for the oxidation is given by the expression $a = a_o e^{-Q/RT}$, where $a_o = 3.2$ and Q = 45,000 cal/mole for pure nickel oxidation over the temperature range 750 - 1240°C.

One may calculate the activation energies for self-diffuison and parabolic oxidation from the data in Figures 3 and 4. The results are tabulated in Tables 2 and 3, respectively. Because the magnitude of the activation energies of the diffusion and the oxidation processes are similar, it is likely that the diffusion process is rate controlling. However, because the oxidation processes are complex chemical reaction, it is difficult to pinpoint which diffusion process controls a specific oxidation process.

Heindlhofer et al.[38] have pointed out that no binary alloy can be expected to oxidize exactly in proportion to the square root of the elasped time at constant temperature, because chemical composition in metals immediately adjacent to the scale changes during that time as a result of selective oxidation and internal oxidation. Although this is true in the early stage of oxidation, after the steady state is established, the concentrations at the oxide/substrate interface may usually be considered constant.[39]

Results obtained by Yao[40] on pure nickel, by Bettridge[29] on Nimonic alloys, and by Kofstad[41] on René 41, Mar-M 200, and IN-100 are shown in Figure 5 with a common unit of ($mg^2/cm^4/sec$) for a parabolic rate constant, a. The parabolic rate constant a decreases in the order of pure nickel ⟶ Nimonic series ⟶ IN 100 ⟶ René 41/Mar-M 200. This order agrees approximately with the alloying effects of Cr, Al, and Ti on oxidtaion, as discussed above.

Under stress or strain, the oxidation reaction will be accelerated because (i) the protective oxide layer is cracked, particularly under a cyclic loading, and (ii) dislocations and surface slip steps are sites of localized high energies where oxidation is accelerated. The effect of applied stress has been studied on several nickel alloys. Oxidation proceeds at an unaffected rate with increasing stress until a critical level of stress is reached, above which oxidation is more rapid. This critical stress to produce accelerated attack is plotted in

Figure 6[42] as a function of exposure temperature for a number of alloys. At the critical applied stress, which generally corresponds to the stress required to produce 1% extension in 100 hours, the rate of metal deformation inhibits the formation of protective and adherent oxide scales. Thus, the continual exposure of fresh metal results in a faster oxidation rate. In this regard, any stress that produces excessive shear at the oxide/metal interface can cause cracking, separating, and exfoliation of the protective oxide and exposure of fresh metal. Creep testing of 10-mil René 41 sheet showed that selective depletion of alloying elements increases significantly with increasing stress.

Rhines et al.[43] have studied the effects of externally applied forces on oxidation rate by suspending high purity nickel tubes in a nickel-tubed furnace with various dead load (tensile stresses: 3050, 6100, 9150, and 12199 psi). The tested tubes were paired, one being stressed and the other unstressed as they were oxidized together in the furnace. Rhines et al. found that as the load is increased, the oxidation rate first diminished both inside and outside the tubes, after which it increases. Antolovich[44] attempted to that account of the effect of stress in terms of the stress dependent diffusion constant for the parabolic kinetics.

Recently, Ikeda et al.[45] studied the effects of strain on the oxidation of stainless steels (Fe- 18 ~ 20Cr, Fe-20Cr-12Ni, and Fe-17Cr-6Ni) in oxygen and in air at 900°C. The oxidtaion of Fe- 18 ~ 20Cr ferritic steels was not accelerated by tensile loadings that produced average strain rates of $10^{-6} \sim 10^{-8}$/sec. However, the oxidation of the austenitic steels was accelerated at the average strain rates of the order of 3×10^{-6}/sec. The authors speculated that the absence of accelerated oxidation in the ferritic steels could be attributed to the rapid diffusion of chromium through these steels and the resulting rapid healing of defects produced in the oxide scale during straining. The low diffusion rate of chromium in the austenitic steels, according to this speculation, did not lead to repair of these defects, and thus, resulted in increasing oxidation during straining.

These observations clearly indicate that engineering materials such as nickel-base superalloys with grain boundaries, carbides, and precipitates should show locally accelerated oxidation, particularly at such microstructural discontinuities, when subjected to an externally applied load and high-temperature oxidation. The spalling and thermal shock resistance in oxides and autogenerated stress in oxides will be discussed in chapter IV.

III. GRAIN BOUNDARY OXIDATION

The grain boundary is an important site for oxidtaion because (i) its composition may differ from that of the matrix, (ii) local disorder may make it chemically more active than the matrix, (iii) it may act as a site for precipitation of harmful or matrix-depleting phases, and (iv) it may function as a rapid diffusion path.[46]

Several interconnected facts on grain boundary oxidtaion appear to be established in the works by Gulbransen et al,[47] Rhodin,[48] Kubaschewski and Hopkins,[49] Cox,[50] and Kofstad.[51] Figure 7(a) illustrates the following phenomena: (i) On a crystal surface, the orientation of the oxide film is directly related to that of the crystal surface. (ii) The rate of growth of such a film depends on its orientation. (iii) On a polycrystalline metal surface, the first layer is randomly oriented and the oxide grains are of different thicknesses owing to the variation in growth rate with orientation. (iv) The oxide films immediately above the grain boundaries or precipitates are thicker than these formed on metal matrix phase.

The rapid oxidation at grain boundaries was observed by Sywestrowicz on titanium thin films.[52] Reporting on the SEM examinations of oxidation characteristics of alloy 800H, Miley et al.[53] found that growth rates of Cr-rich oxide were greatest at the grain boundaries. When external scale had begun to form, the substrate developed with the appearance of oxide particles within the alloy matrix ahead of the interface between metal and external scale by the process of internal oxidation. These internal oxide particles appeared to a greater extent at or near the grain boundaries.[54,55] There also exists a depletion zone of alloying elements at or near the grain boundaries. The oxide particles at the boundaries grew to form continuous films, which progressively enveloped the grains. At the same time, oxidation proceeded within the grain by the formation of further oxide particles ahead of the thickening grain boundary film in much the same way that oxidation occured initially at the metal surface.

Shida et al.,[56] studying preferential intergranular oxides in Ni-Al (0.55 - 4.10%Al) alloys at 800 - 1000°C, identified the several types of intergranular oxide morphologies. They reported that thin and continuous oxides developed along grain boundaries in Ni-0.55Al and Ni-1.5Al and that thick oxide particles developed around and in the boundaries in Ni-2.45Al and Ni-4.10Al at 900 and 1000°C.

Reddy et al.[57] have studied diffusion in Al_2O_3 scales formed on NiCrAl alloys by the proton activation technique employing the O^{18} isotope as a tracer.

They found that the O^{18} profiles identified a zone of oxide penetration beneath the external scale and that oxygen transport was primarily via short-circuit paths such as grain boundaries. Bricknell and his coworkers[3,58,59,60,61] have done extensive work on oxygen embrittlement in Ni and its alloys. Complex oxides were identified on the boundaries at depths roughly an order of magnitude greater than those for matrix internal oxidation.[58,59] Using Auger spectroanalysis, they observed the enhanced O/Ni peak height ratios in the air-exposed (1000°C x 200 hr) samples.[60] However, this technique has disadvantages; (i) the detected O peak cannot distinguish between external oxide and internal oxide, and (ii) this O peak also cannot distinguish inward diffusing oxygen from ambient and dissolved oxygen in the substrate matrix. Therefore, the experimental technique to measure the penetration depth of oxide formed along the grain boundaries has not been well established. The measurement of grain boundary penetration is still based on a conventional technique, examination of the cross section of an oxidized sample under an optical microscope.

Grain size has an effect on the oxidation behavior. Armanet et al.[62] reported on the oxidation behavior of 80Ni-20Cr alloy as a function of average grain size. Depending on the structure, two stages of two different types of gravimetric curves were noted. The first, which is nonparabolic, is due to the growth of a NiO layer over the entire surface of the sample except at grain boundaries, where Cr_2O_3 forms. The second curve is parabolic and is due to the formation of a continuous layer of chromium sesquioxide (Cr_2O_3) at the grain boundaries. The first stage is shorter, and the parabolic stage sets in sooner as the average grain size is smaller. Pischitelli et al.[63] also observed that the oxidation rate in Fe-29Ni-17Co alloy depends on the alloy grain size and the amounts of the minor alloy constituents and that the rate is enhanced at grain boundaries.

As the oxidation process continues, grain boundaries will be preferably oxidized by extended external oxidation or increased internal oxidation, or both, resulting in the morphology shown in Figure 7(b). The outer surface of external oxide scale will be cracked because of thermal and mechanical stresses to be discussed in the next chapter.

Table 4 summarizes the penetration depth of oxide and its thickness along the grain boundary, grain size, and thickness of oxide formed on the surface of various superalloys. This table shows that by prolonging the oxidation process (i) inward oxide penetration may reach two grain sizes in depth and (ii) the

thickness of oxide formed along grain boundaries increases to roughly twice that of the oxide formed on the surface. Therefore, the grain boundary oxide must be crucial for thermomechanical fatigue phenomena (either in crack initiation or in crack propagation). Since the relevant data under unstressed conditions are lacking, it is premature to draw conclusions here. Suffice it to say that stress cycling accelerates the oxidation rate particularly at grain boundaries.

The high-temperature engineering components whose service life limits are controlled by fatigue have been designed to a crack initiation criterion. A component is considered to have failed and is removed from service as soon as a crack reaches the size of 0.031 inch (= 0.8 mm or 800 μm).[64] This critical crack size is comparable to the grain boundary oxide penetration depth in some of the high-temperature alloys shown in Table 4. For longer service times, the penetration depth could conceivably be deeper.

IV. STRESS GENERATION AND ITS EFFECTS ON OXIDATION

During high-temperature oxidation of a metal, internal stresses (called an auto-generated stress) arise from various causes mentioned below. The oxidation behavior will be influenced not only by the externally applied stress but also by this auto-generated internal stress during oxide formation.[65]

An isothermal stress can be attributed to four main causes[66,67]: (i) the epitaxial relationship between the oxide and the metal,[66,68] (ii) the volume ratio between the metal and the oxide formed,[66,67] (iii) composition changes in either the metal or the oxide,[69,70,71,72] and (iv) the influence of vacancies generated during oxidation.[68,73,74,75,76]

It has been stated that stress may arise in oxide films as a result of epitaxial interactions between oxide film and metal substrate. These interactions include oxide/metal lattice mismatch, formation of pores in the oxide and metal and at their interface, and the growth morphology of the oxide.[77,78]

The stress is produced by lattice expansion associated with oxygen solution in the surface layers of the metal, by the volume change that occurs when metal is converted to its oxide at a coherent interface, or by the volume change due to the existence of a substantial gradient in stoichiometry across the oxide.[79] If an oxide film is a coherent and adherent film and if lattice mismatch exists, internal stress will occur. Table 5 lists the volume ratio (ψ), defined as the ratio of the molecular volume of oxide (MeOx) to the atomic volume of metal (Me).[8] Pilling and Bedworth[80] proposed that oxide films could be divided into two classes with regard to their protective abilities by assuming that oxide growth takes place through an inward migration of oxygen through the scale; (i) If the oxide/metal volume ratio is smaller than one (e.g., K_2O, BaO, or MgO), a tensile internal stress will exist in a coherent film, and the oxide will fail to cover the entire metal surface. The oxide will be nonprotective because it is unable to form a coherent surface film, thus continually exposing fresh metal surface. (ii) If the volume ratio is larger than 1, the oxide will be protective except for oxides with extremely high ratios (e.g., Na_2O_5, Ta_2O_5, MoO_3, WO_3, or V_2O_5). These oxides are accompanied by the formation of cracked or porous scales, possibly after an initial stage during which the scale remains coherent.

Even if an ideal situation existed in which the oxide volume and metal volume were equal, it is most likely that each phase would have a different coeffi-

cient of thermal expansion. Thus, if coherene were maintained at all times, interfacial strains would be induced upon any change in temperatures. In general, the thermal dilation is very significant, and the magnitude of the internal stresses is often equal to greater than the fracture stress of the oxides.[65]

If transport occurs by an outward migration of metal by the vacancy mechanism, vacancies may coalesce to form cavities and pores at the metal/scale interface and produce appreciable porosity in the oxide scale after more extended reaction. The porosity is probably due to the development of stresses with subsequent cracking, a phenomenon called breakaway oxidation.[78] Therefore, the oxide that have medium value of volume ratio are more likely to be protective.

In polycrystalline material, large stresses may also develop at the grain boundaries owing to the differences in oxidation rates (i) between neighboring grains and between grains and grain boundaries and (ii) between different crystal surfaces of different orientations.[78] Formation of new phases (such as a spinel-type oxide by a solid-state reaction) during the oxidation reaction may further serve as a source of stress.[81]

An initial compressive stress in the oxide due to epitaxial growth is followed by a period in which the surface regions of the helix were in tension because of vacancy injection into the metal. The net stress may become compressive again as oxidation proceeds.[77] Poole et al.[82] measured the stress in thin films (less than 500 Å thick) of Cu_2O and Fe_2O_3 as compressive stresses of 1.6×10^3 (Kg/cm^2) and 2.7×10^3 (Kg/cm^2), respectively. These stresses, whatever their source, can have a profound effect on film structure. These stresses may cause rupture in the scale.

The internal stresses do not necessarily lead to rupture. During isothermal oxidation at high-temperature, plastic flow and sintering of the oxide may also take place. The stress relief due to plastic deformation of oxide may prevent rupture of the scale. The plastic deformation could be due to slip or could involve high-temperature creep in the oxide.[83] Sintering of the oxide may take place through various diffusion processes such as volume, grain boundary, and surface diffusions, the rates of which all increase exponentially with temperature.[78]

Nonuniform dimensional changes cause internal stresses. These stresses are more significant in oxide films than in bulk metal substrates. Oxides lack ductility to relieve the stress; consequently, cracking and spalling are common in

oxides.[84] Nonuniform dimensional changes may arise from any of the following processes.[84]

(i) Oxide phase transformation

These may be exemplified either by the reconstructive transformation of quartz to cristobalite of SiO_2 or by the displacive transformation of low cristobalite to high cristobalite. Either change invlolves heat-induced expansion, which produces tensile stresses in the unaltered part of the material and compressive stress in the transformed part.

(ii) Differential thermal expansions

These are typified by mullite porcelains ($Al_2O_3 \cdot 2SiO_2$), which exhibit differential expansion in polyphase materials, because mullite has a linear coefficient of 5×10^{-6} cm/cm/^oC, while the surrounding glassy matrix has an expansion coefficient of 7×10^{-6} cm/cm/^oC. Nimonic has linear thermal expansion coefficient of 18×10^{-6} cm/cm/^oC in the temperature range 200 - 1000^oC,[85] while the spinel-type oxide has a linear thermal expansion coefficient of 7.6 - 8.8×10^{-6} cm/cm/^oC in the same temperature range.[86,87]

(iii) Anisotropic thermal expansion within crystals

As an example, an alumina (Al_2O_3) insulator can have adjacent grains that expand 8.3 and 9.0×10^{-6} cm/cm/^oC if their c-axes are perpendicular to each other.

(iv) Temperature differentials and their effect on dimensional changes

Here the simplest example is glass, which might be cooled rather slowly so that the outside layer contracts thermally while the center is still hot and semielastic. A tensile stress exists in the outside layer when the inside is in compression. If the tensile stress in the outside layer causes nonelastic deformation and relieves the tensile stress, and if the glass is further cooled, the center will be in tension and the outside layer will be in compression. Further cooling places the center under tension (and the surface under compression) because the rigid surface cannot continue to contract as the center contracts.

The ways in which intermittent cooling from the service temperature affects weight loss, scale fracture, buckling, and spalling have been widely recognized.[88,89,90,91] Oxide spalling is enhanced by temperature cycling and the thermal-fatigue conditions. A spalling weight loss of 1.0 mg/cm^2 corresponds approximately to a loss of 10^{-4} in./side of metal consumed. Oxide spalling usually exposes an alloy that is depleted in the protective components (Cr and/or Al) so that the

subsequent oxidation rate is faster, with considerable metal being consumed in the process.[42] The potential severity of cyclic versus steady temperature service is illustrated for six commercial alloys in Table 6.[42] These alloys exhibit a wide range of behavior because of the complexity of their reaction products, as well as differing extents of surface and internal oxide attack.

Rapidly forming oxides may have more porosity and larger nonstoichiometry than oxides that form slowly. Hence, a rapidly forming oxide would be more highly stressed and would rupture before reaching the thicknesses observed with slowly forming oxides.[8,37,92] Wolf et al.[92] presented exploratory work on the phenomelogy of gas/metal reactions, considering the anisothermal oxidation of nickel and titanium during heating and when subjected to a variety of controlled heating rates. They used two different heating patterns for anisothermal oxidation; (i) heating rate (1/4 ^{o}C, 4^{o}C, and 8^{o}C/sec.) up to Tm (maximum temperature) of 950^{o}, 1000^{o}, and 1050^{o}C with holding times of 1 and 4 hours, and (ii) after the various heating rates, a cooling rate of 8^{o}C/sec., followed by noholding time at Tm. At a very early stage of isothermal oxidation, the weight gain of the rapidly heated sample (8^{o}C/sec.) was approximately 8 times larger than that heated slowly (0.25^{o}C/sec.). However, after a 1-hr holding time, the ratios of weight losses are reduced to 1 - 1.5.

The role of thermal shock in oxidation weight change in high-temperature alloys was investigated in research conducted at Lewis Research Center.[93] Sheet specimens were oxidized in 1-hr cycles, terminated by slow (1^{o}C/sec.) or fast (240^{o}C/sec.) cooling, to accumulate 100 hours at temperature. Materials were B-1900+Hf, IN-601 (both oxidized at 1100^{o}C), TD-Ni, TD-NiCrAl, IN-702, and Hoskins 875 (oxidized at 1200^{o}C). Records of the progressive weight change are shown in Figure 8. For TD-Ni and Hoskins 875, no oxide spalling was observed under either cyclic condition. For TD-NiCrAl, the shock condition resulted in extensive cracking of the metal and increased oxide loss by spalling. For other materials, slow cooling resulted in greater oxide loss by spalling.

V. MICROSTRUCTURAL CHANGES DUE TO LONG-TERM HEATING

The important time-dependent properties such as creep strength and oxidation depend on the metallurgical structures. The metal temperatures of turbine blade vary between 500°C and 950°C.[94,95] At a high enough service temperature, the metallurgical structures of nickel-base superalloys may change.

Above 0.6Tm (Tm: melting temperature), the γ' phase ($Ni_3(Al,Ti)$) ripens (increases in size) at a significant rate. The higher the γ' particle size, the higher the creep resistance. Therefore, minimizing ripening will help to retain long-term creep resistance,[96] by (i) increasing γ' percent[98] or (ii) adding high-partitioning and slow-diffusing Nb and Ta to the alloy.[96]

Depending on their formability, nickel-base superalloy products are usually used as (i) sheet such as Waspaloy and Rene 41 with 25% γ', (ii) wrought (the strongest) such as Udimet 700 with 35% γ', and (iii) cast such as IN-100 and Mar-M 200 with 55 - 65% γ'.[97] The sheet M-252 of low volume percent γ' has lower flow stress than cast Inconel alloy 700 of high percent γ'. The sensitivity of flow stress to changes in γ' particle size was much greater in the more lean alloys.[96] While a high volume fraction of γ' is desirable for high yield and tensile stresses, the fatigue strength seems to be lowered with increasing volume fraction of γ' particles.[99]

Several general rules can be derived to relate carbide types to alloy compositions after approximately 5000 hours of service. These rules are derived from the computer modelling studies on the formation and decomposition of carbides[100] and long-term (700 to 5000 hours) metallurgical experimental data.[101, 102] The general findings are as follows: (1) Below the critical temperatures of matrix phase stability (815°C), grain boundaries are relatively stable; and MC and $M_{23}C_6$ are the principal equilibrium phases. (2) Low chromium and high columbium, tantalum, molybdenum, tungsten, and iron stabilize MC carbides and improve ductility. (3) At and above 1000°C, Cr_7C_3 has been found only in a basic Ni-Cr-Ti-Al superlalloy such as Nimonic 80A. Addition to the basic superalloy of cobalt (Nimonic 90), molybdenum (Waspaloy), tungsten (D-979), or columbium (Inconel alloy X-750) removes this chromium carbide. (4) At a temperature of 980°C, close to the upper design region, MC, M_6C, and $M_{23}C_6$ are pseudoequilibrium phases in superalloys other than Nimonic 80A. High Cr, Ti, Al, and Ta favor the formation of $M_{23}C_6$; high Mo and W favor M_6C; and Nb and Ta favor MC. (5) As the service

temperature increases, the carbon content of nickel alloys may slowly decrease. After very long exposure, alloy such as Udimet 500 (0.05C) have appeared to lose all MC due to decarbonization.[96]

These microstructural changes (γ'-ripening, carbide-precipitation, and decarbonization) due to long-term exposure at high-temperature may cause different high-temperature low-cycle fatigue or thermomechanical fatigue behaviors. The γ'-ripening causes the decrease of an effective element (Al) for the formation of the protective oxide, and as a result, overall oxidation resistance decreases. Carbide-precipitation provides more crack-initiation sites, to be discussed in the next chapter. Therefore, both microstructural changes may shorten the high-temperature fatigue life in nickel-base superalloys.

The turbine blade alloys are generally heat treated to provide a duplex γ' morphology consisting of large cuboidal precipitates, which confer good creep resistance and small spherical precipitates that increase the tensile strength.[96,103]

The effects of microstructure on elevated temperature fatigue and creep crack growths were studied by Merrick et al.[104] on Waspaloy and P/M Astroloy at 650°C. They reported that in Waspaloy, changes in γ' size and distribution did not markedly affect the fatigue crack growth rate. However, they noticed that an increase in fatigue crack growth rate occurred at low test frequencies and was associated with a transition to intergranular crack propagation. In P/M Astroloy, a coarser grain size lowered the fatigue crack growth rate. Serrated grain boundaries are beneficial under creep loading but have no effect on the fatigue crack growth rate.

There seems to be general agreement, however, that a further complicating factor is that the precipitate structure generally encountered in nickel-base alloy is not stable under stress at elevated temperatures.[4,105] Phase stability, particularly of the precipitates is also related to mechanical stress. Gas-turbine blades made of Ni-alloy E1893 were investigated in the initial state and after 11,000 hours of operation at 730°C.[42] After service the tensile strength increased 10 - 22%, but the ductility and impact strength were reduced 50% because of the aging process.

From the foregoing review of material degradation under the combination of stress and high-temperature oxidation, it is clear that these phenomena may have even more important effects on oxidation behavior at grain boundaries and that this could be crucial to HTLCF (High-Temperature Low-Cycle Fatigue[106])

and TMF (Thermo-Mechanical Fatigue[107]).

VI. HIGH TEMPERATURE FATIGUE CRACK INITIATION AND PROPAGATION

Surface fatigue cracks often originate as intergranular cracks in air at high temperatures, especially at low frequencies. Both environment (particularly oxidation) and time-dependent flow can infuence the propensity for intergranular surface crack initiation, since cracks are often developed as a consequence of the grain boundary sliding, void coalescence, and grain boundary oxidation.[108]

Surface oxidation is detrimental to fatigue because it can cause the formation of stress raisers (such as voids or oxide cracks, as was discussed in chapter IV), and therefore it can accelarate crack inititaion. Paskiet[109] has shown that preoxidation of a specimen at 982°C followed by fatigue testing at 760°C produced many surface intergranular cracks, whereas, testing of specimens without prior oxidation produced a single intergranular crack. Thus, preoxidized phases or grain boundaries served as incipient cracks. Fujita[110] has also proposed a model for accelarated oxidation of surface-connected slip bands, which serve as crack nuclei. Danek[111] and Achter[112] have explained that at high stresses and short fatigue lives, oxygen adsorption at the crack tip accelerates the rate of crack growth in air, while at low stresses, a thicker oxide is formed, which is thought to strengthen the metal.

According to Coffin[113], localized oxidation leads to a "notch" at the surface and localization of the strain, which accelerates further oxidation and sharpens the notch. This reinforcing cycle continues until local fracture occurs. This results in a crack, which they can propagate into the material. It has been seen that the initial region of oxidation is often broad and diffuse, but the notch created by the material removed through oxidation acts to concentrate the deformation further, leading to a wedge-shaped notch and finally a crack. On A286 (iron-base superalloys), Coffin identified highly localized surface oxidation as the nucleation site for fatigue cracks under low-cycle fatigue. Coffin[114] tested A286 and Udimet 500 at 816°C and reported that crack initiation was transgranular in vacuum (10^{-8} torr) and intergranular in air. Therefore, oxidation strongly affects fatigue crack initiation, particularly along grain boundaries.

In fact, it has been generally accepted that in engineering alloys, fatigue crack initiation occurs at some preexisting defect.[115,116] Defects can be micropores that are introduced in casting or atomization, inclusions (both metallic and nonmetallic), and microstructural features such as carbides and brittle second

phases.[117,118] In addition, microstructural features such as grain boundaries, twin boundaries, or precipitates can be crack nucleation sites. In general, defects can be any discontinuity in the microstructure which acts to raise the local stress level. As a result, localized plastic deformation can be generated in regions adjacent to the defects even at a nominal stress well below the yield stress of the material. This localized deformation process is important in fatigue crack initiation.[116] Therefore, the greater the plastic strain concentration, the greater its effect on crack nucleation.

In cast Udimet 500, crack initiation in low-cycle fatigue at 650°C occurs preferentially at surface carbide particles, which cracked during testing.[119] Subsequent crack propagation was found to be in the stage I mode at this temperature. At 815°C, crack initiation occurred preferentially at grain boundaries and interdendritic carbide particles, with subsequent propagation in the stage II mode. At 982°C, fatigue crack initiation takes place totally at grain boundaries.

In the case of columnar and single-crystal Mar-M 200,[120] cracks still originated at the carbides and micropores at 760°C and 927°C. On the other hand, in conventionally cast Mar-M 200, grain boundaries were the preferred sites for crack initiation and propagation at 760°C and 927°C. The mode of propagation in the columnar and single-crystal materials was transgranular. The growth rate was slower and fatigue lives were one or two orders of magnitude higher than those of conventionally cast Mar-M 200, in which cracks grew intergranularly.

Wells et al.[121,122,123] studied Udimet 7000 and found that (i) from the room temperature to 649°C, localization of slip in discrete bands led to slip-band crack initiation at free surfaces, (ii) at 760°C, surface cracking became predominantly intergranular, because of the reduction in grain boundary strength and (iii) at 927°C, crack initiation as well as propagation were intergranular. This observation, in general, agrees with that of Sabol et al.[119]

As temperature increases, indicating of surface intergranular crack initiation have been found in wrought Udimet 700.[122] At 870°C all the crack initiation in this material is at the surface and is intergranular. Often, these intergranular surface cracks propagate only one grain diameter before a transition to transgranular cracking occurs.

Crack initiation has been observed at oxidized carbides at the surface where carbides were decomposed of Inconel 718 tested in air at 850°C.[124]

Fatigue crack was initiated at carbides in René 95.[125]

Antolovich et al.[126] concluded from work on René 80 and René 77 that low-cycle fatigue damage at elevated temperatures is primarily in the form of oxidation or oxide penetration along surface-connected grain boundaries. A crack is said to initiate at a critical degree of boundary penetration, as was discussed in the previous chapter.

Recently, Matsuoka et al.[127] reported that fatigue cracks are initiated at grain boundaries of Fe-9Cr-1Mo steel tested at 593°C and 700°C since the early fracture is intergranular.

Less direct, but nevertheless significant, is the metallographic evidence that crack propagation in air at high-temperature is accompanied by highly localized oxidation on the fracture surface. This, in turn, leads to oxide extrusion, or ridging, as in the case of cast Ni-base superalloys or the formation of complex surface oxide structures as for A 286.[128] Dennison et al.[129] found a similar behavior for cast IN-100, and fatigue fracture occurred by the propagation of surface-nucleated cracks. Romanoski[130] studied high-temperature low-cycle fatigue on René 80 and IN-100 at 871°C and 1000°C and observed that crack initiation and propagation generally occurred at grain boundaries because they possess poorer mechanical strength.

Most alloys when tested at elevated temperatures under cyclic loading, including hold times, usually exhibit a lesser fatigue resistance in terms of cyclic life if the hold is in tension rather than in compression.[130] However, Teranishi et al.[131] found that a compression hold can be more damaging than a tension hold for 2¼Cr-1Mo steel. The reason for the effect of hold time on cyclic life can be related to the behavior of the oxide immediately after the hold time. After a tension hold, the oxide spalls to produce a new surface, which, at least in the early stages of the test, did not contain macroscopic cracks. On the other hand, after a compression hold, the oxide cracks rather than spalls, thereby creating localized stress and strain concentrations. These facilitate the early nucleation of fatigue cracks in the substrate, one of which will ultimately be responsible for failure of the specimen.

Suzuki et al.,[132] using 1Cr-1Mo-¼V steel tested at 500 - 600°C, found that the repeated formation of Fe_2O_3 oxide followed by spalling accelerates the fatigue crack propagation rate. Similar results were obtained by Skelton[133] on Cr-Mo-V steel.

Crack nucleation by oxide ridging at surface grain boundaries has been

observed to be more characteristic of cast Ni-base superalloys at 1600°F (871°C).[134] In all cases, crack nucleation is intergranular, with oxide ridging being the principal mechanism. Propagation, on the other hand, is transgranular at all frequencies (0.03 - 36.2 cpm) tested. This transgranular crack propagation is believed to account for the frequency insensitivity found at high strain and short fatigue lives, through crack tip blunting due to oxidation with decreasing frequency. Transgranular crack growth acts to enhace the resistance of this alloy to fatigue at high-strain low-cycle frequency and hold time.[134]

Among the nickel-base superalloys (IN-100, IN-738, Mar-M 200, René 77, René 80, René 95, Inconel alloy 600, Inconel alloy 718, Udimet 500, and Udimet 700) tested by several researchers cited in this chapter, Inconel alloy 718 and Udimet 500 contain 18 - 19%Cr (see Table 7). This amount of chromium is nearly enough to provide a protective surface oxide film, when a specimen is stress free, as was discussed in chapter II. However, under a cyclic load, cracks are initiated at grain boundaries and propagated intergranularly in Udimet 500 above 815°C[114, 119] and crack initiation is observed at oxidized carbides in Inconel alloy 718 at 850°C.[124] These observations suggest that on material containing about sufficient chromium content for the formation of protective oxide film, such films are not protective against fatigue cycling.

In general, the effects of temperature is to cause an increase in the fatigue crack growth rate, a slight decrease in the threshold ΔK, and a greater sensitivity to frequency effects. At elevated temperatures in air, the cylcic crack growth rates da/dN increase with decreasing frequency. In several nickel-base superalloys, the fatigue crack growth rates range from 2×10^{-5} to 2×10^{-3} in./cycle.[135]

Gell and Duquette[136] interpreted the variations of high-temperature fatigue life in terms of creep-oxidation interaction. They proposed that in the regime of high stresses and short fatigue lives, crack initiation and crack propagation are intergranular because of the high creep component during a fatigue cycle. For tests run in air, oxidation of grain boundary phases accelerates the rates of intergranular crack initiation and propagation and reduces the fatigue life. But, as the stress is lowered, the creep component in a fatigue cycle is reduced, which favors a transgranular mode of cracking and longer fatigue life.[137]

Scarlin[137] has shown that the crack propagation rates for both Nimonic 105 and IN 738LC increased as the cyclic frequency decreased for high-temperature tests in air. The data also showed a higher rate of crack growth in air than in

a vacuum. Scarlin concluded that oxidation was the controlling factor in increasing the propagation rates in air. James[138] has also studied the effect of oxidation on Ni-base superalloys (Inconel 600 ans Inconel 718). Crack growth tests at elevated temperatures were performed in air and in liquid sodium.[139] The growth results showed that crack propagation in liquid sodium was slower than in air, especially in the lower ΔK regime. The decrease in crack growth rate in liquid sodium was associated with the presence of an oxygen free environment.

Recently, Weerasooriya,[140] studying fatigue crack growth rate in IN 718 and IN 100 as a function of temperature (21 - 648°C) and frequency (0.001 - 10 Hz), reported that the fracture surface was entirely covered with oxide and that the color (which is related to the thickness of oxide film) changed continuously depending on temperature and frequency (i.e., oxidation time).

Oxide films are protective if they adhere to the substrate. The film may crack or spall, however, if the sum of the internal and applied stresses exceed the fracture strength of the oxide or the adhesion strength. Both fracture and adhesion strengths can be affected by the temperature, the time at the temperature, and possibly the total accumulated cyclic strain.

Grain boundaries are sites of higher energy, more complex composition, and higher chemical reactivity than the grain matrix. Therefore, the rate of oxidation is faster at the grain boundary than within a grain. Accordingly, the oxide is much thicker in the grain boundary region, and the grain boundaries are the location of potential layer oxide cracks. The nonuniform oxidation rate on the surface of an alloy causes complex internal stresses. Spalling will produce geometric notches in the oxide layer. Both cracks and notches will expose "fresh" substrate material for further oxidation, and the strain localization at the notches and the crack tips will accelerate the crack nucleation process within the matrix material.

Oxidation depletes Al and Cr, which are the major constituents for the γ and γ' strengthening phases. The depletion of Al and Cr weakens the resistance to plastic deformation, including resistance to cyclic plastic deformation, which is one of the principal mechanisms of fatigue crack initiation.

When crack growth during a fatigue cycle $(da/dt)\Delta t$ by the mechanism of oxidation is slower than crack growth by the "regular" cyclic deformation mechanism, then the cyclic crack growth will take over as the major damaging mechanism. Once a crack starts to grow by the cyclic mechanism, the growth rate at high temperature can be accelerated by oxidation and/or creep.

Let us define the cyclic crack growth rate without environmental and creep effects as Δa_f. To affect oxidation, oxygen has to be transported to the crack tip. Let Δa_p be the depth of penetration by the detrimental chemical species, i. e., oxygen. According to Gell et al.,[115] the rate-controlling mechanism is either the surface diffusion of oxygen to the crack tip or the diffusion of oxygen to the region ahead of the crack tip, either through the lattice or along grain boundaries. In addition, the mechanism of direct adsorption and diffusion along slip bands could also be the rate-controlling mechanism.

When $\Delta a_f >> \Delta a_p$, the chemical environment will have a negligible effect on the overall rate of crack growth. This could be the case of low temperature and high cyclic frequency. This is the region of nil-environmental effect, as suggested by Liu and McGowan.[141,142] In this region, the cyclic crack growth rate is not temperature- and frequency-dependent.

When $\Delta a_p >> \Delta a_f$, the detrimental chemical species reaches far ahead of the crack tip. In this case, a crack is propagating in a fully embrittled solid. Again da/dN is not temperature- and frequency-dependent. This is called the fully-environmental effect region.[142] Between these limits, Δa_f is comparable to Δa_p, and da/dN is both temperature- and frequency-dependent. Figure 9 illustrates schematically the fatigue crack growth rate as a function of ΔK, temperature (T), and cyclic frequency (ν).[142]

Cyclic plastic deformation at the crack tip may fracture the oxide film and expose nascent surface for oxidation attack.

When creep accelerates fatigue crack growth, there seems no valid reason for a limit line to which all the crack growth rate data at various temperatures and frequencies converge.

When the cyclic plastic zone size is small relative to the grain size, the crack plane follows specific metallographic planes, crack growth is faceted, and the rate of fatigue crack growth is dependent on crystal orientation and may vary from grain to grain.

Consequently, there are two main competing mechanisms involved in high temperature low-cycle fatigue. To determine which is dominant, a comparison should be made between the crack growth rate (da/dt) during a fatigue cycle by the mechanism of the grain boundary oxidation and the crack growth rate ν(da/dN) by the "regular" cyclic deformation mechanism.

So far, this review has concentrated on general oxidation behavior and localized oxidation (e.g., selective oxidation, internal oxidation, and grain

boundary oxidation) of nickel-base superalloys as well as stress generation and microstructural changes during the oxidation process. It has also been shown that grain boundaries as well as carbides will be sites for fatigue crack initiation, and that grain boundary oxidation has strong effects on not only fatigue crack initiation but also its propagation stage. Figure 10 summarizes the information presented in this review and illustrates the interrelationships among the factors that are important for high-temperature fatigue phenomena.

References

[1a] "Manual on Low Cycle Fatigue Testing" ASTM STP No.465 (1969).

[1b] "Symposium on Fatigue at Elevated Temperature" ASTM STP No.520 (1972).

[1c] Proc. Int'l Conf. on Creep and Fatigue in Elevated Temperature Applications. (1973).

[1d] ASME-MPC-3 Symposium on Creep-Fatigue Interaction (1976).

[2] M.N.Menon and W.H.Reiman;"Low Cycle Fatigue Crack Initiation Study in René 95", AFML-TR-75-1 (July 1975).

[3] R.H.Bricknell and D.A.Woodford; Met. Trans. 12A, 425/433 (1981).

[4] S.D.Antolovich, E.Rosa and A.Pineau; Mat. Sci. and Engr., Feb. (1981).

[5] L.F.Coffin, Jr.; Trans. ASM, 56, 339/344 (1963).

[6] C.J.McMahon and L.F.Coffin, Jr.; Met. Trans. 1, 3443/3450 (1970).

[7] O.Kubaschewski and B.E.Hopkins; "Oxidation of Metals and Alloys", 130, Butterworths, London (1962).

[8] ibid., 8/12.

[9] ibid., 129.

[10] P.Kofstad; "High Temperature Oxidation of Metals", 274, John-Wiley & Sons, NY (1966).

[11] ibid., 285.

[12] ibid., 13/14.

[13] ibid., 292.

[14] R.B.Herchenroeder, G.Y.Lai and K.V.Rao; Jour. of Metals, 35, 16/22 (1983).

[15] E.A.Gulbransen and S.A.Jansson; "Thermochemistry of Gas-Metal Reactions", in "Oxidation of Metals and Alloys", ASM, Ohio, 86 (1971).

[16] P.Goldsmith, F.G.May and R.D.Wiffen; Nature, 210, 475 (1968).

[17] G.C.E.Olds; "Metals and Ceramics", 67/68, Pliver & Boyd, Edinburgh (1968).

[18] G.C.Wood and T.Hodgkiess; Nature (London), 211, 685 (1966).

[19] M.G.Fontana and N.D.Greene; "Corrosion Engineering", 364/365, McGraw-Hill Book Comp., NY (1967).

[20] A.Davin and D.Coutsouadis; "What are the effects of alloying elements singly or in combination on hot corrosion?", 221/233 in AGARD Conf.Proc. No.120, in "High Temperature Corrosion of Aerospace Alloys" ed. by J.Stringer, R.I.Jaffee and T.F.Kearns.

[21] C.S.Giggins and F.S.Pettit; Trans. AIME, 245, 2509 (1969).

[22] C.C.Smith and P.Pean; Bristol-Siddeley Engineers Lab. Rep. No. 452 (1966).

[23] R.M.Schirmer and H.T.Quigg; Prog. Rep. on NASC Cont. No. 65-0310-d (1966).

[24] R.F.Decker and C.T.Sims; "The Metallurgy in Nickel-Base Alloys", 33/37 in "The Superalloys" ed. by C.T.Sims and W.C.Hagel, John-Wiley & Sons, NY (1972).

[25] W.Betteridge; "Nickel and its Alloys", 35, MacDonald & Evans, Plymouth (1977).

[26] S.M.Copley, B.H.Kear and F.L.VerSnyder; "The Role of Interfaces in Ni-Base Superalloys", 353/369 in "Surfaces and Interfaces II" Proc. of the 14th Sagamore Army Materials Research Conf., ed. by J.J.Burke, N.L.Reed and V.Weiss, Syracuse University Press (1968).

[27] A.R.Coex et al.; "Application of Rapidly Solidified Superalloys", Report FR-9744, Pratt & Whitney Aircraft (Feb. 1978).

[28] H.H.Uhlig; "Corrosion and Corrosion Protection", 172, John-Wiley & Sons, NY (1967).

[29] W.Bettridge; "Nickel and its Alloys", 43/44, MacDonald & Evans, Plymouth (1977).

[30] R.G.Frank and W.F.Zimmerman; "Materials for Rockets and Missiles", 21, MacMillian Comp. (1959).

[31] S.T.Wlodek; Trans. Met. Soc. AIME, 230, 177/185 (1964).

[32] G.W.Goward; Jour. of Metals, 31/39 (1970).

[33] R.A.Rapp and D.A.Shores; Tech. of Met. Rev. IV, pt.2, Wiley. NY, 159/160 (1970).

[34] O.Kubaschewski, E.L.Evans and C.B.Alcock; "Metallurgical Thermochemistry" Pergamon Press, NY (1967).

[35] C.Wagner; Z.Physik. Chem (B), 21, 35 (1932).

[36] O.Kubaschewski and H.E.Hopkins; "Oxidation of Metals", 35/36, Butterworths, London (1962).

[37] ibid., 10.

[38] K.Heindlhofer and B.M.Larson; Trans. Amer. Soc. Steel Treat., 21, 865 (1933).

[39] O.Kubaschewski and H.E.Hopkins; "Oxidation of Metals", 114, Butterworths, London (1962).

[40] Y.L.Yao; J.Phys. Chem., 33, 741 (1960).

[41] P.Kofstad; "Nonstoichiometry, Diffusion, and Electrical Conductivity in Binary Metal Oxides", 101/362, Wiley-Interscience, NY (1972).

[42] G.E.Wasielewski and R.A.Rapp; "High-Temperature Oxidation" in "The Superalloys" ed. by C.T.Sims and W.C.Hagel, 287/316, John-Wiley & Sons, NY (1972).

[43] F.N.Rhines and R.G.Connel, Jr.; "Influence of Stress Upon the High Temperature Oxidation of Nickel" in "Stress Effects and the Oxidation of Metals" ed. by J.C.Cathcart, AIME, 94/113 (1975).

[44] S.D.Antolovich; "Metallurgical Aspects of High Temperature Fatigue" presented at Int'l Summer School "Fatigue in Materials and Structures" in Sherbrooke, Canada (1978).

[45] Y.Ikeda and K.Ni; Jour. Japan Inst. Metals, 47, 191/197 (1983) (in Japanese).

[46] J.Stringer; in "Grain Boundaries in Engineering Materials", 445/459, Proc. 4th Bolton Landing Conf., Claitor's Pub (1974).

[47] E.A.Gulbransen; Industr. Engng. Chem., 41, 1385 (1949).

[48] T.N.Rhodin; Jour. Amer. Chem. Soc., 72, 5102 (1950) and 73, 3143 (1951).

[49] O.Kubaschewski and H.E.Hopkins; "Oxidation of Metals", 63, Butterworths, London (1962).

[50] B.Cox; J.Electrochem. Soc., 108, 24 (1961).

[51] P.Kofstad; "High Temperature Oxidation of Metals", 186, John-Wiley & Sons, NY (1966).

[52] W.D.Sylwestrowicz; J.Electrochem. Soc., 122, 1504/1508 (1975).

[53] D.V.Miley and G.R.Smolik; Edgerton, Germeshausen and Grier, Inc., Idaho (1981).

[54] O.Kubaschewski and H.E.Hopkins; "Oxidation of Metals", 138, Butterworths, London (1962).

[55] J.Benard and J.Moreau; Rev. Metall., 47, 317 (1950).

[56] Y.Shida, F.H.Stott, G.C.Wood, B.D.Bastow and D.P.Whittle; Oxidation of Metals, 18, 93/113 (1982).

[57] K.P.R.Reddy, A.R.Cooper and J.L.Smialek; Oxidation of Metals, 17, 429/449 (1982).

[58] D.A.Woodford and R.H.Bricknell; Met. Trans., 12A, 1467/1475 (1981).

[59] R.H.Bricknell and D.A.Woodford; Met. Trans., 12A, 1673/1680 (1981).

[60] R.H.Bricknell, D.A.Woodford and R.A.Mulford; Met. Trans., 13A, 1223/1232 (1982).

[61] R.H.Bricknell and D.A.Woodford; in "Creep and Fracture of Engineering Materials and Structures" Proc. Int'l Conf., Swansea, Pineridge Press, 249/262 (1981).

[62] P.Moulin, P.Lacombe and F.Armanet: Memoires Scientifiques de la Revue de Metallurgie, 74, 143/160 (1977).

[63] R.A.Pischitelli, S.K.Rhee and F.N.Bradley; J.Electrochem. Soc., 123, 929/933 (1976).

[64] S.A.Sattar and C.V.Sundt; Jour. of Aircraft, 12, 360/365 (1975).

[65] D.L.Douglas; "Exfoliation and the Mechanical Behavoir of Scales" in "Oxidation of Metals and Alloys" ASM, 137/156 (1971).

[66] P.Hancock; "The Role of Stress During Oxidation" in "High Temperature Corrosion of Aerospace Alloys" ed. by J.Stringer, R.I.Jaffee and T.K.Kearns, AGARD Conf. Proc., No.120, 117/128 (1973).

[67] J.Stringer; Corr. Sci., 10, 513/543 (1970).

[68] A.T.Fromhold, Jr., "Stress and Strain in Growing Oxide Films" in "Stress Effects and the Oxidation of Metals" ed. by J.V.Cathcart, AIME, 2/74 (1975).

[69] O.Richmond; Trans. ASM, 57, 294 (1964).

[70] R.E.Pawel and J.J.Campbell; Acta. Met., 14, 1827 (1966).

[71] R.E.Pawel and J.J.Campbell; J.Electrochem. Soc., 116, 828 (1969).

[72] V.R.Howes and C.N.Richardson; Corr. Sci., 9, 385 (1969).

[73] P.Hancock and R.Fletcher; Metallurgie, 6, 1 (1966).

[74] W.Jaenicke et al.; J.Electrochem. Soc., 111, 1031 (1964).

[75] W.K.Appleby et al.; Corr. Sci., 10, 325 (1970).

[76] C.S.Giggins, E.J.Felten and F.S.Pettit; "Growth Stress Induced Features of Al_2O_3 Scales Developed on Alloys During Oxidation" in "Stress Effects and the Oxidation of Metals" ed. by J.V.Cathcart, AIME, 245/261 (1975).

[77] B.S.Borie et al.; Acta. Met., 10, 691 (1962).

[78] P.Kofstad; "High Temperature Oxidation of Metals", 230/234, John-Wiley & Sons, NY (1966).

[79] J.V.Cathcart; "The Structure and Properties of Thin Oxide Films", 27 in "Oxidation of Metals and Alloys", ASM (1971).

[80] N.B.Pilling and R.E.Bedworth; J.Inst.Metals, 29, 529 (1923).

[81] W.W.Smeltzer: Acta. Met., 8, 268 (1960).

[82] P.Poole and L.L.Shreir; Electrochem. Acta., 13, 269/276 (1968).

[83] C.S.Tedmon, Jr., J. Electrochem. Soc., 114, 788 (1967).

[84] L.H.VanVlack; "Physical Ceramics for Engineers", 140/166, Addison-Wesley Pub., Reading (1964).

[85] W.Bettridge; "Nickel and its Alloys", 58/59, MacDonald & Evans (1977).

[86] W.D.Kirgery, H.K.Bowen and D.R.Uhlman; "Introduction to Ceramics", 583, John-Wiley & Sons, NY (1976).

[87] J.D.Filby; "Oxides as Substrates in Microelectronics", 222 in "Modern Oxide Materials Preparation, Properties and Design Applications" ed.by B.Cockayne and D.W.Jones, Academic Press, London (1972).

[88] C.H.Wells, P.S.Follansbee and R.R.Dils; "Mechanisms of Dynamic Degradation of Surface Oxides" 220/244 in "Stress Effects and the Oxidation of Metals" ed. by J.V.Cathart, AIME (1975).

[89] D.L.Douglas; Oxidation of Metals, 1, 127/142 (1969).

[90] C.E.Lowell and H.B.Probst; "Effects of Composition and Testing Conditions on Oxidation Behavior of Four Cast Commercial Nickel-Base Superalloys", NASA Technical Note TN D-7705 (1974).

[91] D.Bruce and P.Hancock; Jour. Inst. of Metals, 97, 148/155 (1969).

[92] J.S.Wolf and J.M.Grochowski; "The Nature of Gas-Metal Reactions Under Conditions of Anisothermal Oxidation", 274/297 in "Stress Effect and the Oxidation of Metals" ed. by J.V.Cathcart, AIME (1974).

[93] C.E.Lowell and D.L.Deadmore; "The Role of Thermal Shock in Cyclic Oxidation" Report NASA TM-78876 (1978).

[94] J.E.Restall; "The Environment Encountered High-Temperature Components of the Aircraft Gas Turbine" 15/29 in AGARD Conf. Proc. "High Temperature Corrosion of Aerospace Alloys" ed. by J.Stringer, R.I.Jaffee and T.F.Kearns, (1973).

[95] R.A.Sigmorelli, J.R.Johnston and J.W.Weeton; "Evaluation of a Cast Nickel-Base Alloy for Use as a Bucket Materials at 1650°F", 33 in "High Temperature Materials" ed. by R.F.Hehemann and G.H.Ault, Jown-Wiley & Sons, (1959).

[96] R.F.Decker and C.T.Sims; "The Metallurgy in Nickel-Base Alloys", 33/37 in "The Superalloys", ed. by C.T.Sims and W.C.Hagel, John-Wiley & Sons, (1972).

[97] A.W.Thompson and I.M.Bernstein; "The Role of Metallurgical Variables in Hydrogen-Assisted Environmental Fracture" 55/175, in "Advances in Corrosion Science and Technology Vol.7" ed. by M.G.Fontana and R.W.Staehle, (1980).

[98] E.Bartlett; "Superalloys" 7/8 in CAB Current Awareness Bulletin No.112 (1982).

[99] N.S.Stoloff; "Fundamentals of Strengthening", 107 in "The Superalloys" ed. by C.T.Sims and W.C.Hagel, John-Wiley & Sons, (1972).

[100] R.F.Decker; "Strengthening Mechanisms in Nickel-Base Superalloys", Climax Molybdenum Company Syposium, Zurich (May, 1969).

[101] H.E.Collins; "Relative Stability of Carbide and Intermetallic Phases in Nickel-Base Superalloys" Int'l Sym. on Structural Stability in Superalloys, Seven Springs, PA (1968).

[102] E.L.Raymond; Trans. AIME, 239, 1415 (1967).

[103] O.H.Kriege and J.M.Baris; Trans. ASM, 62, 195/200 (1969).

[104] H.F.Merrick and S.Floreen; Met. Trans. 9A, 231/236 (1978).

[105] J.K.Tien and S.M.Copley; Met. Trans. 2, 543/553 (1971).

[106] S.D.Antolovich, S.Liu and R.Baur; Met. Trans. 12A, 473/481 (1981).

[107] R.C.Bill, M.J.Verrilli, M.A.McGaw and G.R.Halford; "A Preliminary Study of the Thermomechanical Fatigue of Polycrystalline Mar-M 200", Lewis Research Center, NASA (1983).

[108] L.F.Coffin, Jr., S.S.Manson, A.E.Carden, L.K.Severud and W.L.Greenstreet; "Time-Dependent Fatigue of Structural Alloys", ORNL-5073 (Jan. 1977).

[109] G.F.Paskiet, D.H.Boone and C.P.Sullivan; J.Inst. of Metals, 100, 58 (1972).

[110] F.E.Fujita; "Fracture of Solids" 657, Interscience Publ., NY (1963).

[111] G.J.Danek, Jr., H.H.Smith and M.R.Achter; Proc. ASTM, 61, 775 (1961).

[112] M.R.Achter; Proc. Inst. Environt. Sci., 385 (1963).

[113] L.F.Coffin , Jr.; Trans. ASM, 56, 339/344 (1963).

[114] L.F.Coffin , Jr.; Int'l Conf. on Corrosion Fatigue (1971).

[115] M.Gell and G.R.Leverant; "Fatigue at Elevated Temperature" ASTM STP 520 (1973).

[116] J.C.Grosskretz; "Metal Fatigue Damage" ASTM STP 495 (1971).

[117] J.M.Hyzak; "The Effect of Defects on the Fatigue Initiation Process in Two P/M Superalloys" AFML-TR-80-4063 (Sep. 1980).

[118] J.M.Hyzak and I.M.Bernstein; Met. Trans., 13A, 33/43 (1982).

[119] G.P.Sabol, T.F.Herrgstenberg and D.M.Moon; "Electron Microscopy and Structure of Metals" 753/763 ed. by G.Thomas et el., Univ. Calif. Press (1972).

[120] G.R.Leverant and M.Gell; Trans. AIME, 245, 1167 (1969).

[121] C.H.Wells and C.P.Sullivan; Trans. ASM, 58, 391 (1965).

[122] C.H.Wells and C.P.Sullivan; Trans. ASM, 60, 217 (1967).

[123] C.H.Wells and C.P.Sullivan; Trans. ASM, 61, 149 (1968).

[124] L.F.Coffin , Jr.; Met. Soc. AIME, 1/23 (1980).

[125] M.N.Menon and W.H.Reiman; J. of Materials Science, 10, 1571/1581 (1975).

[126] S.D.Antolovich, P.Domas and J.L.Strudel; Met. Trans.,10A, 1859/1868 (1979).

[127] S.Matsuoka, S.Kim and J.R.Weertman; "Mechanical and Microstructural Behavior of a Ferritic Stainless Steel under High Temperature Cycling", 69, Proc. ASM Fall Meeting (Phil. 1983).

[128] D.A.Woodford and L.F.Coffin, Jr.; "The Role of Grain Boundaries in High-Temperature Fatigue", General Electric Company R & D Technical Information Series Class 1 Report No. 74CRD 180 (Aug. 1974).

[129] J.P.Dennison, P.D.Holmes and B.Wilshire; Met. Sci. and Engr., 33, 35/47 (1978).

[130] G.R.Romanoski, Jr; "Mechanisms of Deformation and Fracture in High-Temperature Low-Cycle Fatigue of Rene 80 and IN 100", NASA Contractor Report 165498 (March 1982).

[131] H.Teranishi and A.J.McEvily; Met. Trans., 10A, 1806/1808 (1979).

[132] M.Suzuki, Y.Iino, M.Muramatsu, Y.Sasabuchi and K.Wada; Materials, 31, 717/722 (1982). (in Japanese)

[133] R.P.Skelton; Mat. Sci. Engr., 35, 297 (1978).

[134] L.F.Coffin, Jr.; Met. Trans., 5, 1053/1060 (1974).

[135] H.D.Solomon and L.F.Coffin , Jr.; "The Effect of frequency and environment on fatigue crack growth in A286 at 1000°F" ASTM STP 520, 112/122 (1972).

[136] M.Cell and D.J.Duquette; Corrosion Fatigue, NACE,2, 366 (1972).

[137] R.B.Scarlin; "Fracture 77", 2, 849, Pergamon Press, NY (1977).

[138] W.J.Mills and L.A.James; J. Engr. & Tech. Trans. ASME, 101, 205 (1979).

[139] L.A.James and R.L.Knecht; Met. Trans. 6A, 109 (1975).

[140] T.Weerasooriya; "Micro-Mechanics of Crack Growth in Two Nickel-Base Superalloys", 31, Proc. ASM Fall Meeting (phil. 1983).

[141] H.W.Liu and J.J.McGowan; Scripta Met., 15, 507/512 (1981).

[142] J.J.McGowan and H.W.Liu; Trans. ASME, 103, 246/252 (1981).

[143] L.F.Coffin, Jr.; "Fatigue at High Temperature -Prediction and Interaction" James Clayton Lecture, Proc. Instn. Mech. Engrs., 188, 109/127 (1974).

Table 1 Heats of decomposition of individual oxide of alloying elements in Nickel-base alloys [8]

metal	oxide	ΔH_{dec} [Kcal]
Ni	NiO	115.0
Cr	Cr_2O_3	180.0
Co	CoO	114.2
Mo	MoO_2	140.6
	MoO_3	77.6
W	WO_2	140.9
	WO_3	134.1
Ta	Ta_2O_5	195.6
Nb (Cb)	Nb_2O_5	146.8
Al	Al_2O_3	266.8
Ti	TiO_2	176.2
Fe	FeO	126.5
	Fe_3O_4	144.5
	Fe_2O_3	110.2
minor alloying element		
Si	SiO_2	210.2
Zr	ZrO_2	259.5
V	V_2O_5	60.0

Table 2

activation energy for self-diffusion, -Q [Kcal/mole]

system	calculated from fig. 3	ref. data
Co/CoO	40	34.5
Ni/NiO	50	56
Cr/$NiCr_2O_4$	80	72.3
Ni/$NiCr_2O_4$	90	74.5
Co/$CoCr_2O_4$	95	51
Cr/$CoCr_2O_4$	95	70
Cr/Cr_2O_3	120	100
Al/Al_2O_3	120	

Table 3

activation energy for high temperature oxidation, -Q [Kcal/mole]

material	calculated Q from fig. 4	weight % Cr	Co	Mo	Al	Ti	Nb
In-100	53	10	15	3	5.5	4.5	—
René 41	69	19	11	10	1.5	3.1	—
René Y	51						
INCO 713	87	12.5	—	4.2	6.1	0.8	2
Mar-M 200							
<1700°F	37	9	10	—	5	2	1 + 12W
>1700°F	180						
U-700	100	15	18.5	5.2	4.3	3.5	—

Table 4

material	condition	penetration depth of oxide (μm) :PDO	grain size (μm) :GS	PDO/GS	Crack in oxide : CIO CIO/PDO	grain boundary oxide thickness (μm) :GBO	surface oxide thickness (μm) :SO	GBO/SO	source
René 77	927°C 100 hr $\Delta\varepsilon_p$=0.12%	25	40 ∿ 65	0.4 ∿ 0.6	1	2.5	1.25	2	[44]
René 80	982°C 100 hr $\Delta\varepsilon_p$=0.07%			1.0 ∿ 1.4	1			1	[44]
René 80	871°C $\Delta\varepsilon_p$=0.25%	50	30	1.7	1	3 ∿ 4	1	3 ∿ 4	[106]
Udimet 500	816°C	236	120	2.0	1	20	10	2	[143]
René 80	1000°C								[135]
	17 hr	100	150 ∿ 200	0.5 ∿ 0.6	1	15	15	1	
	37 hr	40	40	1.0	1	8	8	1	
	56 hr	370	154	2.4	1	30	30	1	
IN 100	925°C								
	7 hr	80	40 ∿ 50	1.6 ∿ 2.0	1	13	9	1.4	
	87 hr	120	50 ∿ 80	1.5 ∿ 2.4	1	10	6	1.7	

Table 5 Volume ratio of oxides [8]

metal	oxide	volume ratio (ψ) = $\frac{\text{molecular volume of oxide}}{\text{atomic volume of metal}}$
K	K_2O	0.45
Ba	BaO	0.67
Mg	MgO	0.81
Cr	Cr_2O_3	2.07
M	MO_2	2.10
W	WO_2	2.08
Fe	Fe_2O_3	2.14
	Fe_3O_4	2.10
Co	CoO	1.86
Ni	NiO	1.65
Al	Al_2O_3	1.54
Ti	TiO_2	1.80
Zr	ZrO_2	1.50
Nb	Nb_2O_5	2.68
Ta	Ta_2O_5	2.46
Mo	MoO_3	3.30
W	WO_3	3.35
V	V_2O_5	3.19

Table 6 Effects of cyclic air oxidation on spalling (400 hr at 1100°C) [42]

Alloy	Static Exposure		Cyclic Exposure[a]	
	Spalled Oxide (mg/cm^2)	Total Affected[b] Metal (mil/side)	Spalled Oxide (mg/cm^2)	Total Affected[b] Metal (mil/side)
René 80	15.2	7.3	101.0	12.9
IN-100	3.0	4.6	8.7	12.5
713C	2.7	1.8	36.8	9.5
Hastelloy X	0.5	2.5	3.4	4.0
René Y	0	1.8	0.07	2.0
TD Ni-Cr	0	0.8	0.3	1.0

[a] 16-25 hr cycles to room temperature.

[b] Includes metal that converted to oxide and IO (internal oxides)

Table 7 Chemical compositions of Nickel-base superalloys (w/o)

Alloy Designation	Nominal Composition, Weight %															
	Ni	Cr	Co	Mo	W	Ta	Cb	Al	Ti	Fe	Mn	Si	C	B	Zr	Other
Nickel-Base																
Alloy 713C	74	12.5	-	4.2	-	-	2.0	6.1	0.8	-	-	-	0.12	0.012	0.10	
Alloy 713LC	75	12.0	-	4.5	-	-	2.0	5.9	0.6	-	-	-	0.05	0.010	0.10	
B-1900	64	8.0	10.0	6.0	-	4.0	-	6.0	1.0	-	-	-	0.10	0.015	0.10	
FORD 406	60	6.0	10.0	1.0	8.5	6.0	2.0	4.5	2.0	-	-	-	0.13	0.018	0.06	
IN-100/René 100	60	10/9.5	15.0	3.0	-	-	-	5.5	4.7/4.2	-	-	-	0.18	0.014	0.06	1.0V
IN-162	73	10.0	-	4.0	2.0	2.0	1.0	6.5	1.0	-	-	-	0.12	0.020	0.10	
IN-731	67	9.5	10.0	2.5	-	-	-	5.5	4.6	-	-	-	0.18	0.015	0.06	1.0V
IN-738	61	16.0	8.5	1.7	2.6	1.7	0.9	3.4	3.4	-	-	-	0.17	0.010	0.10	
IN-792	61	12.4	9.0	1.9	3.8	3.9	-	3.1	4.5	-	-	-	0.12	0.020	0.10	
M22	71	5.7	-	2.0	11.0	3.0	-	6.3	-	-	-	-	0.13	-	0.60	
MAR-M 200	60	9.0	10.0	-	12.0	-	1.0	5.0	2.0	-	-	-	0.15	0.015	0.05	
Mar-M 200(DS)	60	9.0	10.0	-	12.0	-	1.0	5.0	2.0	-	-	-	0.13	0.015	0.05	
MAR-M 246	60	9.0	10.0	2.5	10.0	1.5	-	5.5	1.5	-	-	-	0.15	0.015	0.05	
MAR-M 421	61	15.8	9.5	2.0	3.8	-	2.0	4.3	1.8	-	-	-	0.15	0.015	0.05	
MAR-M 432	50	15.5	20.0	-	3.0	2.0	2.0	2.8	4.3	-	-	-	0.15	0.015	0.05	
NX188(DS)	74	-	-	18.0	-	-	-	8.0	-	-	-	-	0.04	-	-	
RENE' 77	58	14.6	15.0	4.2	-	-	-	4.3	3.3	-	-	-	0.07	0.016	0.04	
RENE' 80	60	14.0	9.5	4.0	4.0	-	-	3.0	5.0	-	-	-	0.17	0.015	0.03	
SEL	51	15.0	22.0	4.5	-	-	-	4.4	2.4	-	-	-	0.08	0.015	-	
SEL-15	58	11.0	14.5	6.5	1.5	-	0.5	5.4	2.5	-	-	-	0.07	0.015	-	
TAZ-8A	68	6.0	-	4.0	4.0	8.0	2.5	6.0	-	-	-	-	0.12	0.004	1.00	
TRW-NASA VIA	61	6.1	7.5	2.0	5.8	9.0	0.5	5.4	1.0	-	-	-	0.13	0.020	0.13	0.5Re,0.4Hf
UDIMET 500	52	18.0	19.0	4.2	-	-	-	3.0	3.0	-	-	-	0.07	0.007	0.05	
WAZ-20(DS)	72	-	-	-	20.0	-	-	6.5	-	-	-	-	0.20	-	1.50	

	Ni	Cr	Co	Mo	W	Ta	Cb	Al	Ti	Fe	Mn	Si	C	B	Zr	Other
Nickel-Base																
Astroloy	55.1	15.0	17.0	5.25	-	-	-	4.0	3.5	-	-	-	0.06	0.030	-	-
D-979	45.0	15.0	-	4.0	4.0	-	-	1.0	3.0	27	-	-	0.05	0.010	-	-
Hastelloy alloy X	47.3	22.0	1.5	9.0	0.6	-	-	-	-	18.5	0.50	0.50	0.10	-	-	-
Inconel alloy 600	76.6	15.8	-	-	-	-	-	-	-	7.2	0.20	0.20	0.04	-	-	-
Inconel alloy 601	60.7	23.0	-	-	-	-	-	1.35	-	14.1	0.50	0.25	0.05	-	-	-
Inconel alloy 625	61.1	22.0	-	9.0	-	-	4.0	0.2	0.2	3.0	0.15	0.30	0.05	-	-	-
Inconel alloy 706	41.5	16.0	0.5	0.5	-	-	2.9	0.2	1.75	40.0	0.18	0.18	0.03	-	-	-
Inconel alloy 718	53.0	18.6	-	3.1	-	-	5.0	0.4	0.9	18.5	0.20	0.30	0.04	-	-	-
Inconel alloy X-750	73.0	15.0	-	-	-	-	0.9	0.8	2.5	6.8	0.70	0.30	0.04	-	-	-
IN-102	67.9	15.0	-	3.0	3.0	-	3.0	0.4	0.6	7.0	-	-	0.06	0.005	0.03	0.02Mg
IN-587	47.2	28.5	20.0	-	-	-	0.7	1.2	2.3	-	-	-	0.05	0.003	0.05	-
IN-597	48.4	24.5	20.0	1.5	-	-	1.0	1.5	3.0	-	-	-	0.05	0.012	0.05	0.02Mg
IN-853	74.6	20.0	-	-	-	-	-	1.5	2.5	-	-	-	0.05	0.007	0.07	1.3Y_2O_3
M-252	55.2	20.0	10.0	10.0	-	-	-	1.0	2.6	-	0.50	0.50	0.15	0.005	-	-
Nimonic alloy 75	78.8	20.0	-	-	-	-	-	-	0.4	-	0.10	0.70	0.01	-	-	-
Nimonic alloy 80A	74.7	19.5	1.1	-	-	-	-	1.3	2.5	-	0.10	0.70	0.06	-	-	-
Nimonic alloy 90	57.4	19.5	18.0	-	-	-	-	1.4	2.4	-	0.50	0.70	0.07	-	-	-
Nimonic alloy 105	53.3	14.5	20.0	5.0	-	-	-	1.2	4.5	-	0.50	0.70	0.20	-	-	-
Nimonic alloy 115	57.3	15.0	15.0	3.5	-	-	-	5.0	4.0	-	-	-	0.15	-	-	-
Nimonic alloy PE.11	39.0	18.0	1.0	5.25	-	-	-	0.85	2.35	33.5	-	-	0.05	-	-	-
Nimonic alloy PE.16	43.5	16.5	1.0	3.3	-	-	-	1.2	1.2	33.0	0.10	0.15	0.05	0.020	-	-
Nimonic alloy PK.33	55.9	18.5	14.0	7.0	-	-	-	2.0	2.0	0.25	0.10	0.15	0.05	0.030	-	-
Nimonic alloy 120	63.8	12.5	10.0	5.7	-	-	-	4.5	3.5	-	-	-	0.04	-	-	-
Nimonic alloy 942	49.5	12.5	1.0	6.0	-	-	-	0.6	3.9	27.5	-	-	0.03	-	-	-
Pyromet 860	43.0	12.6	4.0	6.0	-	-	-	1.25	3.0	30.0	0.05	0.05	0.05	0.010	-	-
RA-333	45.0	25.5	3.0	3.0	3.0	-	-	-	-	18.0	1.50	1.20	0.05	-	-	-
René 41	55.3	19.0	11.0	10.0	-	-	-	1.5	3.1	-	-	-	0.09	0.005	-	-
René 95	61.3	14.0	8.0	3.5	3.5	3.5	-	3.5	2.5	-	-	-	0.15	0.010	0.05	-
TD Nickel	98.0	-	-	-	-	-	-	-	-	-	-	-	-	-	-	2.0ThO_2
TD NiC	78.0	20.0	-	-	-	-	-	-	-	-	-	-	-	-	-	2.0ThO_2
Udimet 500	53.6	18.0	18.5	4.0	-	-	-	2.9	2.9	-	-	-	0.08	0.006	0.05	-
Udimet 520	56.9	19.0	12.0	6.0	1.0	-	-	2.0	3.0	-	-	-	0.05	0.005	-	-
Udimet 700	53.4	15.0	18.5	5.2	-	-	-	4.3	3.5	-	-	-	0.08	0.030	-	-
Udimet 710	54.9	18.0	15.0	3.0	1.5	-	-	2.5	5.0	-	-	-	0.07	0.020	-	-
Unitemp AF2-1DA	59.5	12.0	10.0	3.0	6.0	1.5	-	4.6	3.0	-	-	-	0.32	0.015	0.10	-
Waspaloy	58.3	19.5	13.5	4.3	-	-	-	1.3	3.0	-	-	-	0.08	0.006	0.06	-

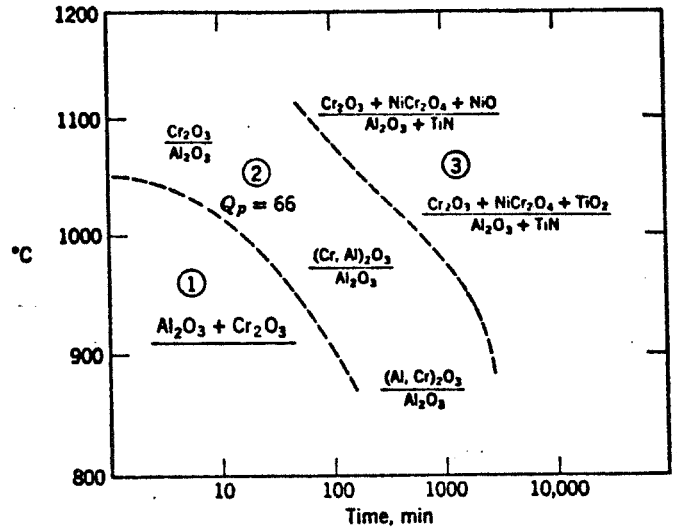

(a) René-41

19%Cr, 11%Co, 10%Mo, 3.1%Ti, 1.5%Al, 0.7%Fe

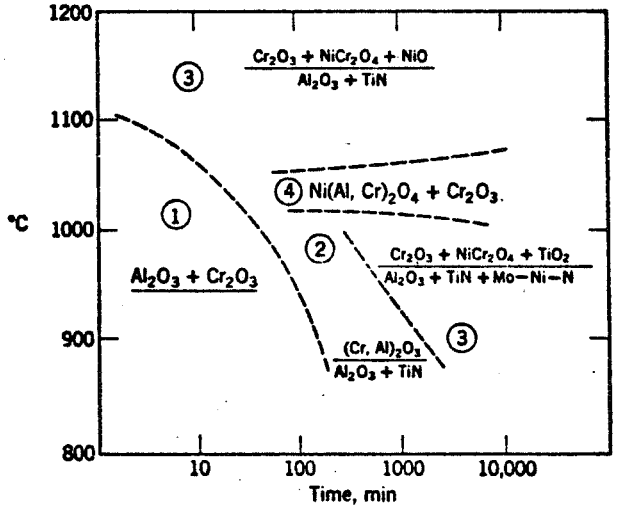

(b) Udimet-700

15%Cr, 19%Co, 5%Mo, 3.5%Ti, 4.5%Al

Note: i) phases in the numerators represent the external scale,
ii) phases in the denominator represent the internal scale,
(1) represents the linear oxidation region,
(2) and (3) represent the parabolic oxidation regions, and
(4) represents a constant weight region after 1000 min.

Fig. 1 Schematic representation of reaction products formed as a function of time and temperature in air oxidation [10]

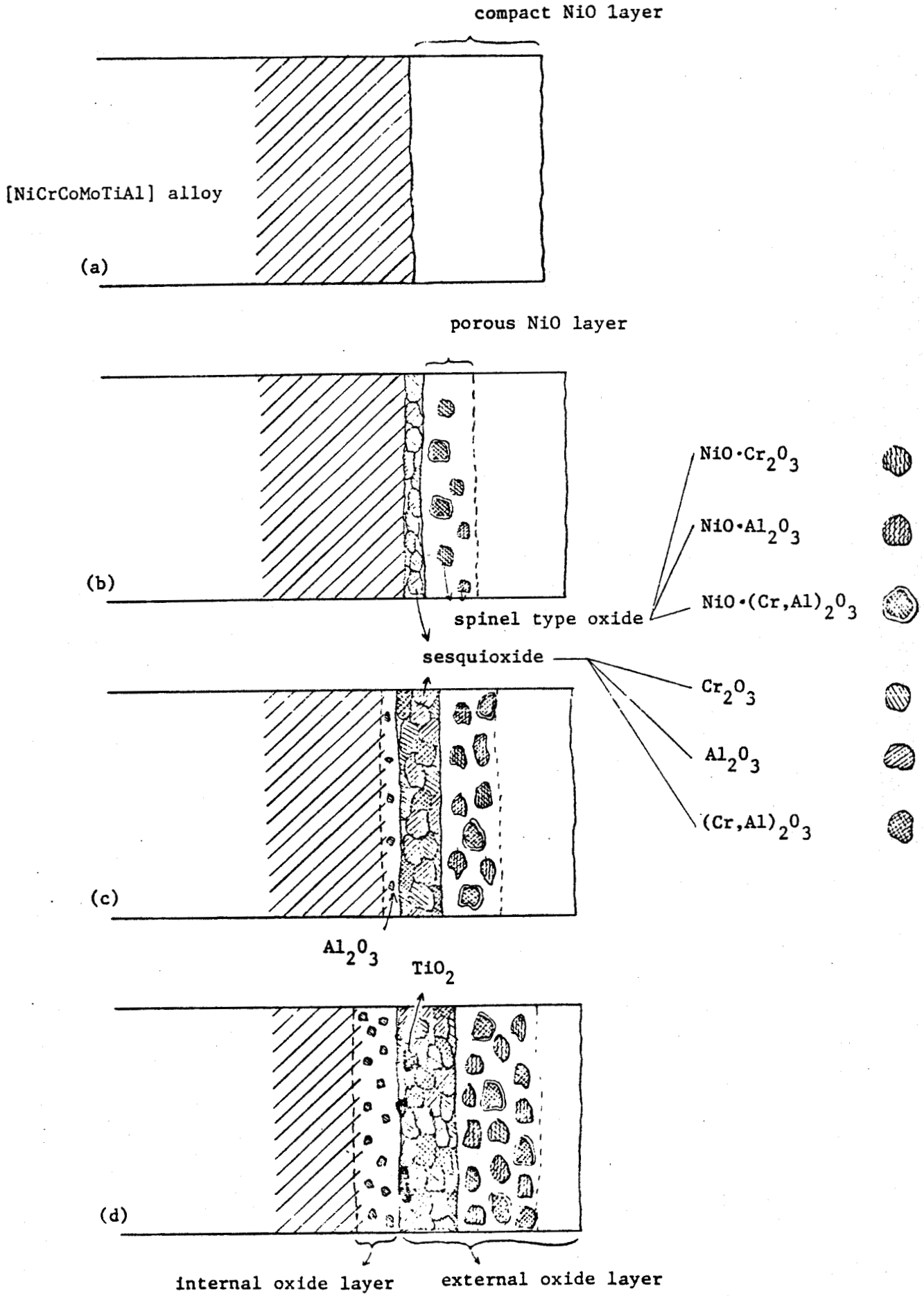

Fig.2 Schematic illustrations for complex oxides formation on Nickel-base superalloys

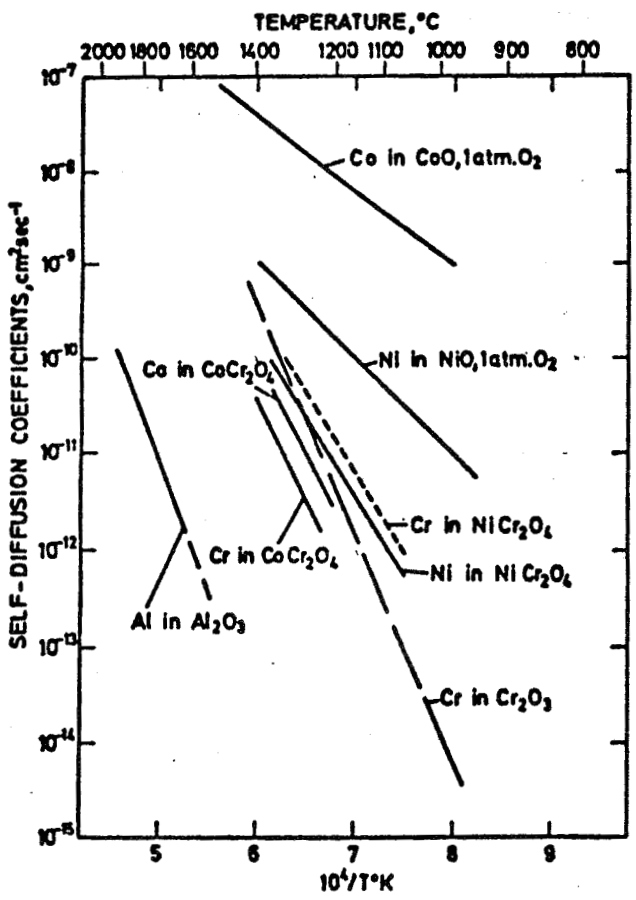

(a)

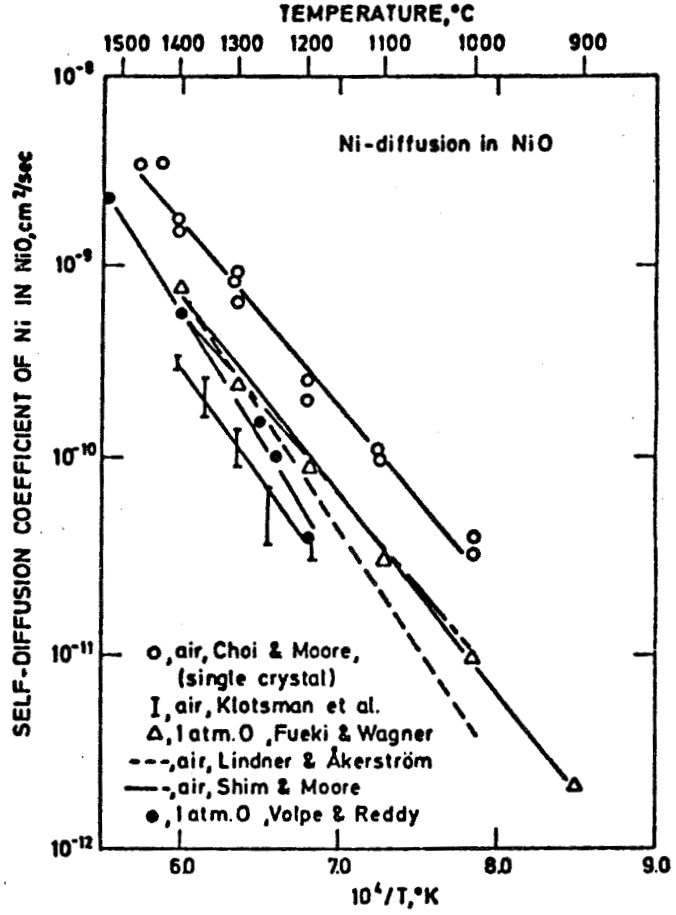

(b)

Fig.3 Self-diffusion coefficients of the cations in oxides [41]

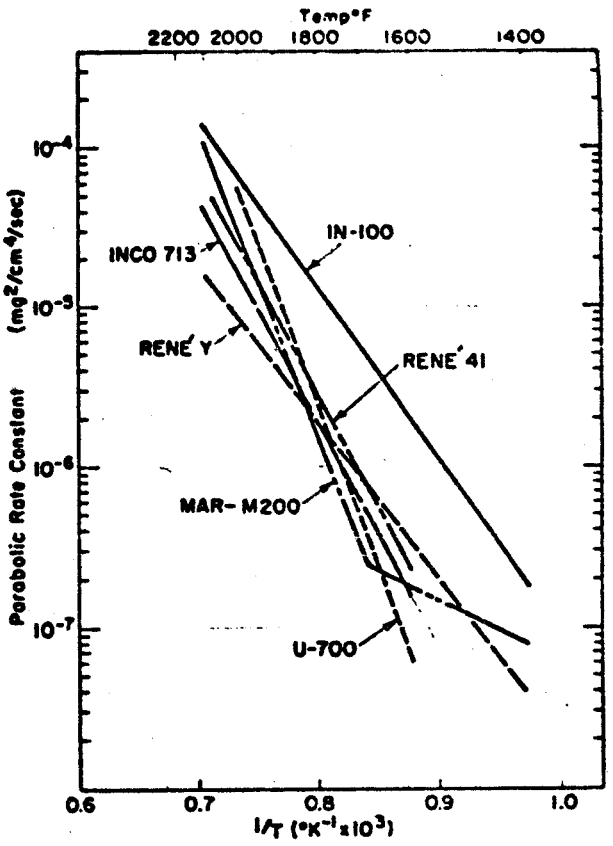

Fig.4 Parabolic rate constants for oxidation on several Ni-base superalloys

[41]

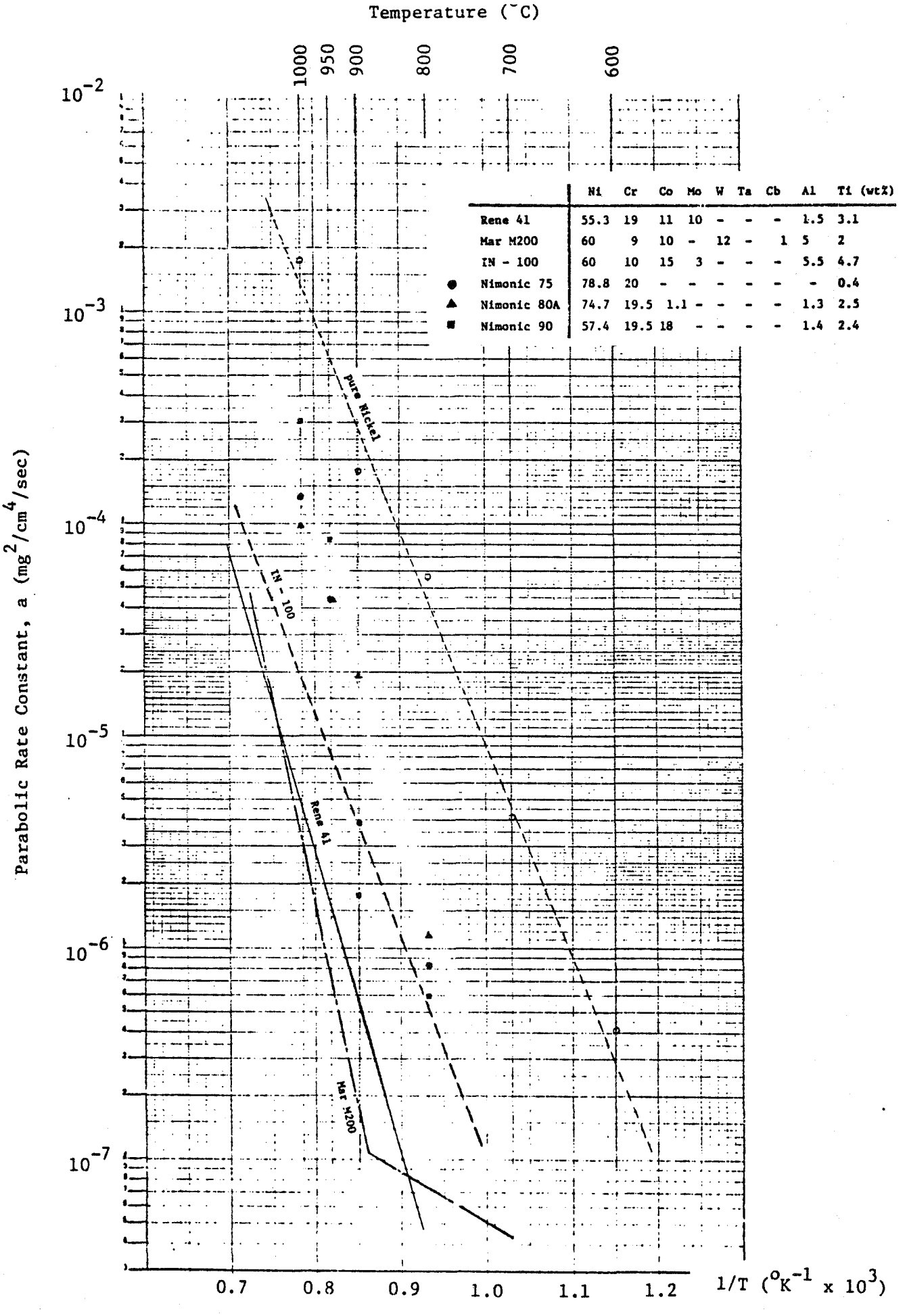

	Ni	Cr	Co	Mo	W	Ta	Cb	Al	Ti (wt%)
Rene 41	55.3	19	11	10	-	-	-	1.5	3.1
Mar M200	60	9	10	-	12	-	1	5	2
IN - 100	60	10	15	3	-	-	-	5.5	4.7
● Nimonic 75	78.8	20	-	-	-	-	-	-	0.4
▲ Nimonic 80A	74.7	19.5	1.1	-	-	-	-	1.3	2.5
■ Nimonic 90	57.4	19.5	18	-	-	-	-	1.4	2.4

Fig.5 Parabolic rate constants for oxidation on several Ni-base superalloys

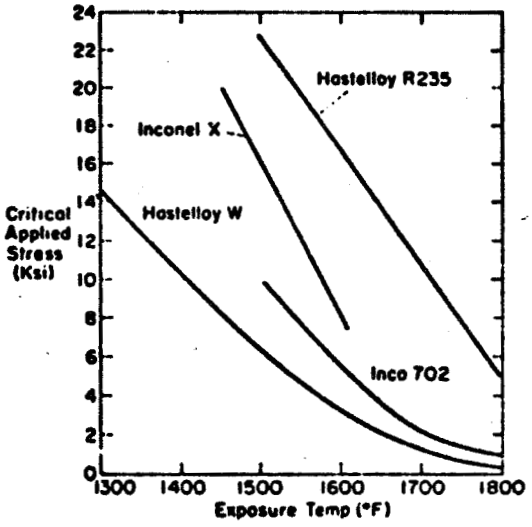

Fig.6 The critical applied stress required to produce acceleration oxidation as a function of exposure temperature for Ni-base superalloys [42]

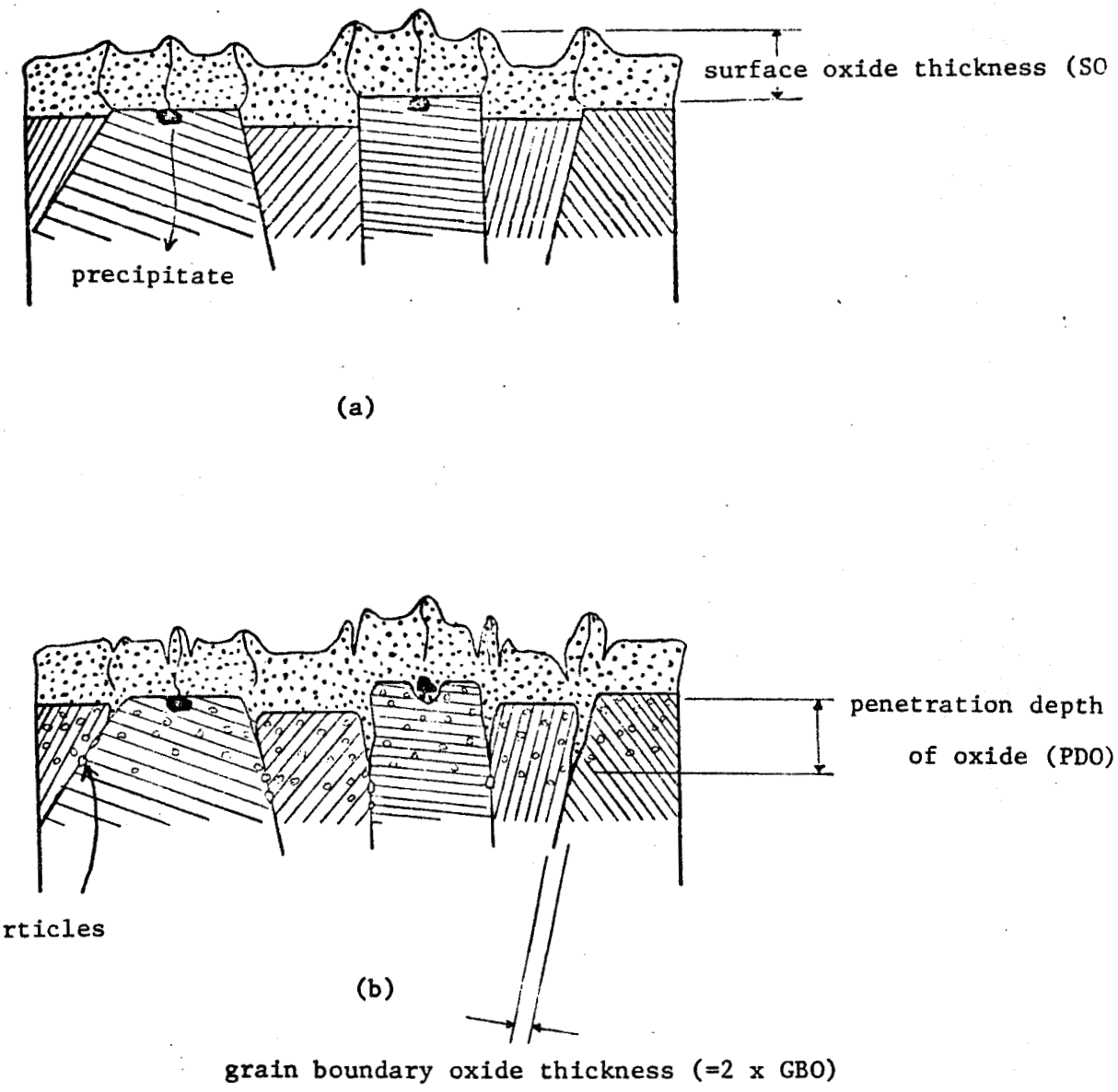

Fig.7 Schematic illustrations for oxide growth in cross-sectional view

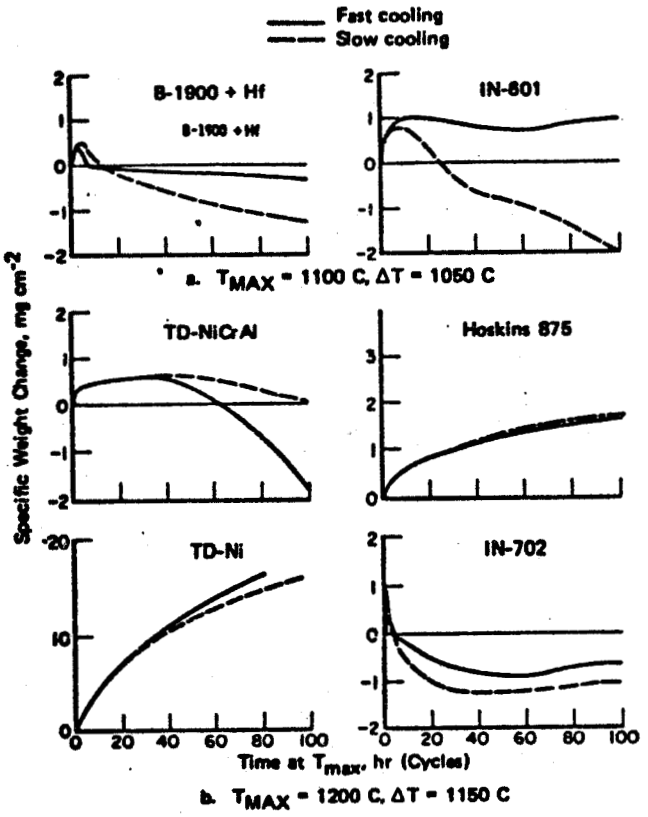

Fig.8 The effect of cooling rate on the cyclic oxidation of some high-temperature alloys

Note: 1 hr at T_{max} and 0.5 hr at T_{min} per cycle [93]

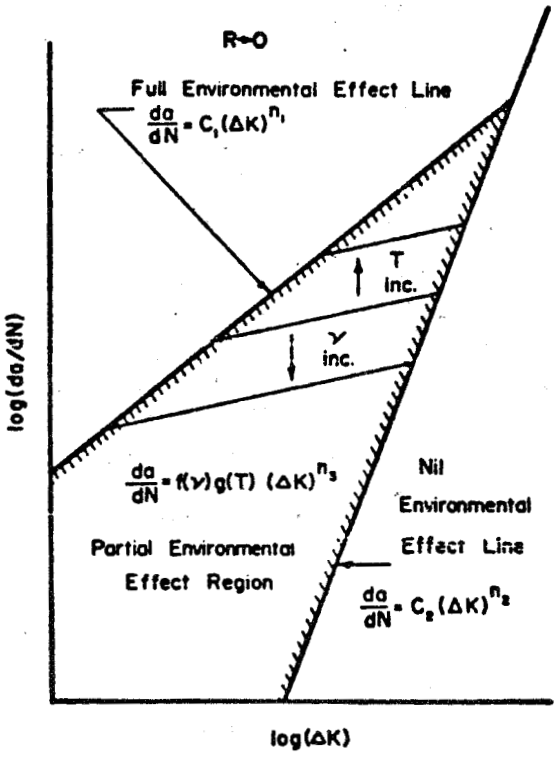

Fig. 9 Cyclic crack growth model schematic.

[143]

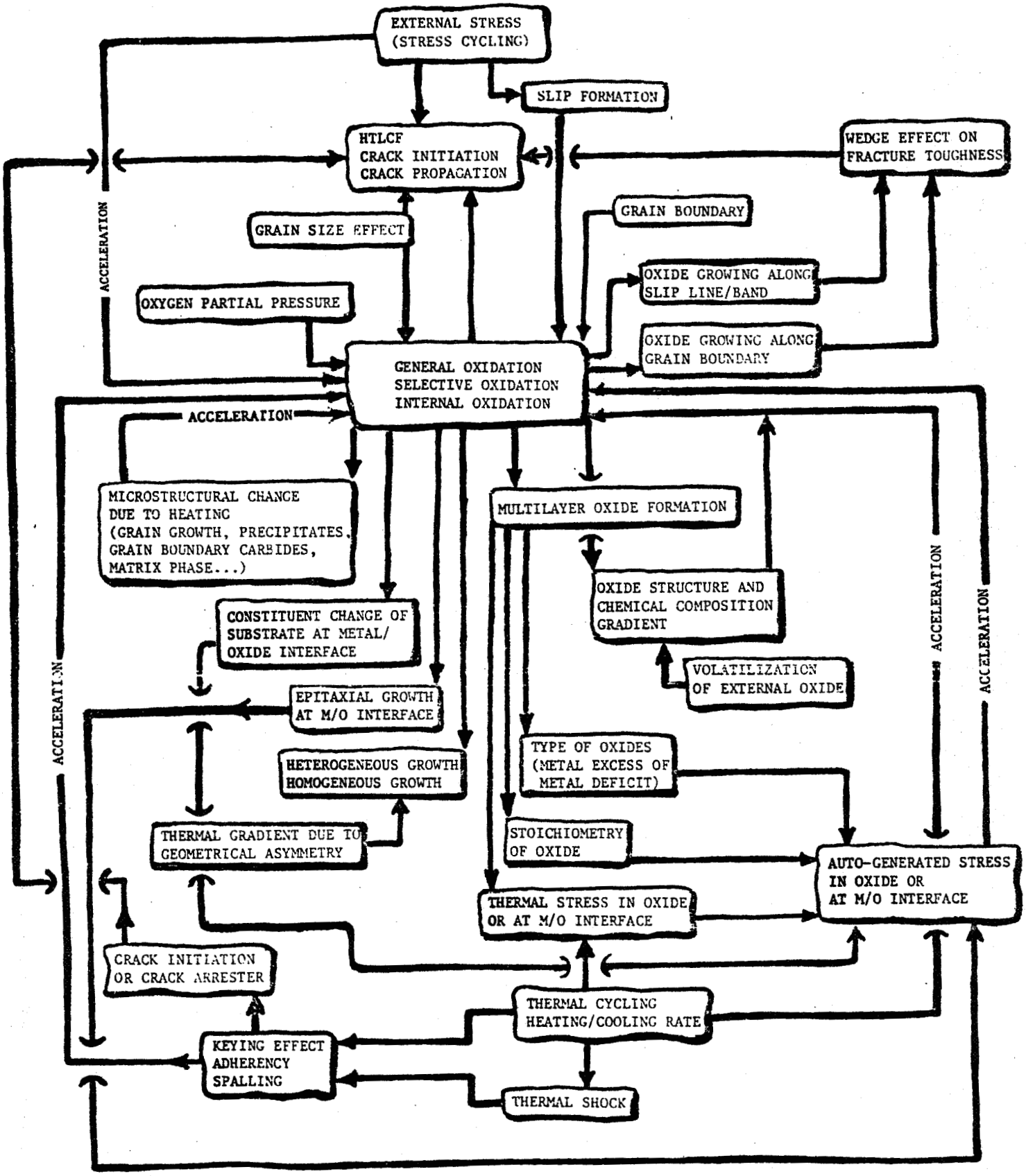

Fig.10 Interrelationships among various important factors for high temperature low cycle fatigue

1. Report No.	2. Government Accession No.	3. Recipient's Catalog No.
NASA CR-174639		

4. Title and Subtitle	5. Report Date
Literature Survey on Oxidations and Fatigue Lives at Elevated Temperatures	March 1984
	6. Performing Organization Code
7. Author(s)	8. Performing Organization Report No.
H. W. Liu and Y. Oshida	None
	10. Work Unit No.
9. Performing Organization Name and Address	11. Contract or Grant No.
Syracuse University Dept. of Chemical Engineering and Materials Science Syracuse, New York 13210	NAG 3-348
	13. Type of Report and Period Covered
12. Sponsoring Agency Name and Address	Contractor Report
National Aeronautics and Space Administration Washington, D.C. 20546	14. Sponsoring Agency Code 505-33-22

15. Supplementary Notes

Final report. Project Manager, John L. Shannon, Jr., Structures and Mechanical Technologies Division, NASA Lewis Research Center, Cleveland, Ohio 44135.

16. Abstract

Nickel-base superalloys are the most complex and the most widely used for high-temperature applications such as aircraft engine components. The desirable properties of nickel-base superalloys at high temperatures are tensile strength, thermomechanical fatigue resistance, low thermal expansion, as well as oxidation resistance. At elevated temperature, fatigue cracks are often initiated by grain boundary oxidation, and fatigue cracks often propagate along grain boundaries, where the oxidation rate is higher. Oxidation takes place at the interface between metal and gas. Properties of the metal substrate, the gaseous environment, as well as the oxides formed all interact to make the oxidation behavior of nickel-base superalloys extremely complicated. The important topics include general oxidation, selective oxidation, internal oxidation, grain boundary oxidation, multi-layer oxide structure, accelerated oxidation under stress, stress-generation during oxidation, composition and substrate microstructural changes due to prolonged oxidation, fatigue crack initiation at oxidized grain boundaries and the oxidation accelerated fatigue crack propagation along grain boundaries. These factors are reviewed in this report.

17. Key Words (Suggested by Author(s))	18. Distribution Statement
Superalloys; Oxidation; Fatigue; Crack initiation; Crack propagation	Unclassified - unlimited STAR Category 26

19. Security Classif. (of this report)	20. Security Classif. (of this page)	21. No. of pages	22. Price*
Unclassified	Unclassified	51	A04

*For sale by the National Technical Information Service, Springfield, Virginia 22161